© 2014. Published by The Company of Biologists Ltd | Journal of Cell Science (2014) 127, 5164–5178 doi:10.1242/jcs.147744

RESEARCH ARTICLE

Clustered PI(4,5)P_2 accumulation and ezrin phosphorylation in response to CLIC5A

Abass Al-Momany[1], Laiji Li[2], R. Todd Alexander[3] and Barbara J. Ballermann[1,2,*]

ABSTRACT

CLIC5A (encoded by *CLIC5*) is a component of the ezrin–NHERF2–podocalyxin complex in renal glomerular podocyte foot processes. We explored the mechanism(s) by which CLIC5A regulates ezrin function. In COS-7 cells, CLIC5A augmented ezrin phosphorylation without changing ezrin abundance, increased the association of ezrin with the cytoskeletal fraction and enhanced actin polymerization and the formation of cell surface projections. CLIC5A caused the phosphatidylinositol 4,5-bisphosphate [PI(4,5)P_2] reporter RFP–PH-PLC to translocate from the cytosol to discrete plasma membrane clusters at the cell surface, where it colocalized with CLIC5A. Transiently expressed HA–PIP5Kα colocalized with GFP–CLIC5A and was pulled from cell lysates by GST–CLIC5A, and silencing of endogenous PIP5Kα abrogated CLIC5A-dependent ERM phosphorylation. N- and C-terminal deletion mutants of CLIC5A, which failed to associate with the plasma membrane, failed to colocalize with PIP5Kα, did not alter the abundance of PI(4,5)P_2 plasma membrane clusters and failed to enhance ezrin phosphorylation. Relative to wild-type mice, in CLIC5-deficient mice, the phosphorylation of glomerular ezrin was diminished and the cytoskeletal association of both ezrin and NHERF2 was reduced. Therefore, the mechanism of CLIC5A action involves clustered plasma membrane PI(4,5)P_2 accumulation through an interaction of CLIC5A with PI(4,5)P_2-generating kinases, in turn facilitating ezrin activation and actin-dependent cell surface remodeling.

KEY WORDS: Phosphatidylinositol 4,5-bisphosphate, ezrin, ERM protein, Chloride intracellular channel, CLIC, Podocyte, Glomerular

INTRODUCTION

The chloride intracellular channel (CLIC) 5A belongs to a family of highly conserved redox-sensitive metamorphic proteins distantly related to glutathione-S-transferase (Cromer et al., 2002; Littler et al., 2004). CLICs exist as soluble, membrane-bound or cytoskeleton-associated forms and exhibit ion-conducting properties in artificial phospholipid bilayers (Ashley, 2003; Berryman et al., 2004). Whether CLICs function as specific Cl^- channels in cells is uncertain, given that antagonists of classic Cl^- channels, 4,4′-diisothiocyanatostilbene-2,2′-disulfonate (DIDS) and 4-acetamido-4′-isothiocyanato-2,2′-stilbenedisulfonic acid (SITS) have no effect on CLIC channel activity. Nonetheless, the inhibitor indanyloxyacetic acid 94 (IAA-94), originally used to isolate p64, the bovine CLIC5B isoform, reduces ion conductance of CLICs (Ashley, 2003; Landry et al., 1993; Redhead et al., 1992; Tulk et al., 2000). CLICs are found in diverse subcellular locations, for instance at the base of actin-based microvilli and stereocilia (Berryman and Bretscher, 2000; Gagnon et al., 2006; Salles et al., 2013), the Golgi, mitochondria and secretory vesicles (Berry et al., 2003; Chuang et al., 1999; Fernández-Salas et al., 1999; Redhead et al., 1992; Shanks et al., 2002). Their mechanism(s) of action are as yet incompletely understood.

Two alternative first exons (A and B) of the *CLIC5* gene produce the 32-kDa isoform CLIC5A (251 amino acids) and the 49-kDa CLIC5B (410 amino acids), respectively (Berryman and Bretscher, 2000; Shanks et al., 2002). CLIC5A was first discovered in a protein complex isolated from human placental microvilli, together with ezrin and several other actin-associated proteins (Berryman and Bretscher, 2000). When CLIC5A was overexpressed in cells, it localized to microvilli and a substantial portion became resistant to detergent extraction and remained coupled to the cytoskeleton (Berryman et al., 2004). In the inner ear, CLIC5A colocalizes with actin at the base of cochlear and vestibular hair cell stereocilia, with a similar distribution to that of the ERM (ezrin, radixin and moesin) protein radixin (Gagnon et al., 2006; Salles et al., 2013). In CLIC5-deficient mice ($CLIC5^{jbg/jbg}$), CLIC5A is absent from the cochlear and vestibular hair cells, radixin expression is reduced and stereocilia degenerate after birth, leading to vestibular dysfunction and complete deafness by 7 months of age (Gagnon et al., 2006; Salles et al., 2013), a phenocopy of radixin deficiency (Kitajiri et al., 2004).

We previously reported that CLIC5A mRNA is highly expressed and enriched in human renal glomeruli compared with its expression in other tissues and cells (Nyström et al., 2009). In glomeruli, CLIC5A colocalizes with ezrin and podocalyxin in a highly polarized fashion at the apical plasma membrane of podocyte foot processes. In mice lacking CLIC5A, transmission electron microscopy shows broadening and patchy fusion of podocyte foot processes, and ezrin as well as phospho-ezrin levels are reduced relative to those of wild-type mice (Pierchala et al., 2010; Wegner et al., 2010). These findings suggest that CLIC5A is required for the development and maintenance of the ezrin-dependent ultrastructural organization of glomerular podocyte foot processes, akin to the dependence of stereocilia integrity on CLIC5A in cochlear and vestibular hair cells.

ERM proteins function to link integral plasma membrane proteins to cortical F-actin (Bretscher, 1999; Tsukita and Yonemura, 1999). They play a crucial role in defining cell morphology and processes like adhesion, migration and endocytosis (Bretscher et al., 2002; Denker and Barber, 2002;

[1]Department of Physiology, University of Alberta, Edmonton, AL T6G 2V2, Canada. [2]Department of Medicine (Nephrology), University of Alberta, Edmonton, AL T6G 2V2, Canada. [3]Department of Pediatrics, Faculty of Medicine and Dentistry, University of Alberta, Edmonton, AL T6G 2V2, Canada.

*Author for correspondence (barbara.ballermann@ualberta.ca)

Received 7 December 2013; Accepted 3 September 2014

Journal of Cell Science

Journal of Cell Science (2014) 127, 5164–5178 doi:10.1242/jcs.147744

Denker et al., 2000; Ivetic and Ridley, 2004; Takeuchi et al., 1994). ERM proteins play a crucial role in the formation of actin-based cellular extensions like microvilli, filopodia, microspikes, lamellipodia and podocyte foot processes (Baumgartner et al., 2006; Lamb et al., 1997; Schwartz-Albiez et al., 1995; Takeuchi et al., 1994). They are involved in signal transduction pathways (Tsukita and Yonemura, 1997) and in cancer cell metastasis (Khanna et al., 2004; Machesky, 2008). In their inactive state, intramolecular associations mask the N- and C-ERM association domains (ERMAD), rendering ERM proteins unable to bind to integral membrane proteins or F-actin. Inactive ERM proteins remain cytosolic and are unstable (Grune et al., 2002). Interaction of the ERM protein N-terminus with phosphatidylinositol 4,5-bisphosphate [PI(4,5)P_2] in lipid bilayers releases the inhibitory interaction between N- and C-termini and supports subsequent phosphorylation of a conserved C-terminal threonine (Thr) residue (Thr567 in ezrin, Thr564 in radixin and Thr558 in moesin) (Fievet et al., 2004). Activation of ERM proteins increases their stability and enables interaction of the N-ERMAD with integral membrane proteins and the C-ERMAD with F-actin (Bretscher et al., 2002; Ivetic and Ridley, 2004; Yonemura et al., 2002). Several kinases, including protein kinase C (PKC), MRCK and AKT can directly phosphorylate PI(4,5)P_2-anchored ERM proteins (Ivetic and Ridley, 2004; Shiue et al., 2005). Rho kinase (ROCK) can also phosphorylate ERM proteins *in vitro* (Hirao et al., 1996), but in cells ERM phosphorylation is not blocked by ROCK inhibition (Matsui et al., 1999).

In this study, we used the simple model of ectopically expressed CLIC5A in COS-7 cells, which do not express CLIC5A at baseline, to determine whether CLIC5A regulates ezrin function. Ectopically expressed CLIC5A increases PI(4,5)P_2 production in dorsal plasma membrane clusters through a functional interaction with PI(4,5)P_2-generating kinases, in turn facilitating ezrin phosphorylation, its association with the actin cytoskeleton and the formation of cell surface projections. These data suggest that CLIC5A promotes localized PI(4,5)P_2 generation, thus stimulating ezrin protein activation.

RESULTS

Increased ERM protein phosphorylation in COS-7 cells expressing CLIC5A

Given that CLIC5A deficiency results in reduced ezrin and phosphorylated (phospho)-ERM abundance in glomerular podocytes of CLIC5$^{jbg/jbg}$ mice (Wegner et al., 2010), and dephosphorylated ERM proteins are unstable (Grune et al., 2002), we hypothesized that CLIC5A regulates ezrin phosphorylation. To investigate this, COS-7 cells, which lack detectable CLIC5A, were transiently transfected with pcDNA3.1-CLIC5A or with empty vector and evaluated for ERM phosphorylation. Although total ezrin levels were similar in CLIC5A- and vector-transfected cells, ERM protein phosphorylation was greater in SDS lysates of

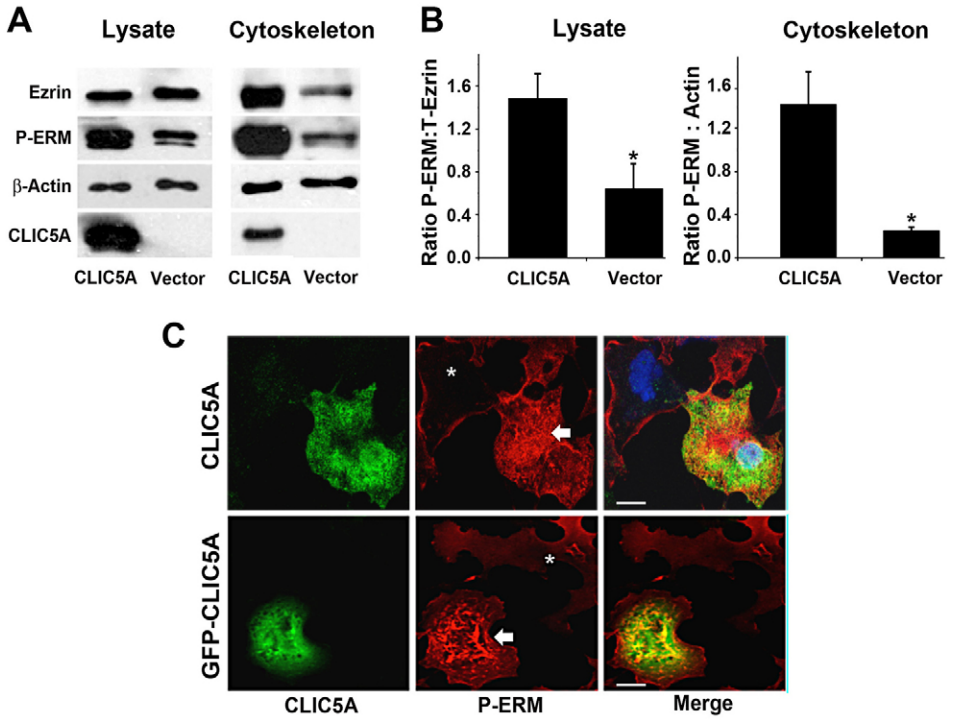

Fig. 1. Increased ERM phosphorylation in COS-7 cells transfected with CLIC5A. (A) Western blot analysis of total SDS-soluble proteins (Lysate) and solubilized cytoskeletons prepared from COS-7 cells transfected with CLIC5A cDNA or vector alone. Blots were probed with rabbit anti-ezrin, mouse anti-phospho-ERM (P-ERM), mouse anti-β-actin and rabbit anti-CLIC5A antibodies. (B) Densitometric determination of the ratio of phospho-ERM:total ezrin (T-Ezrin) in total SDS-solubilized lysates and the ratio of phospho-ERM:actin in solubilized cell cytoskeletons from COS-7 cells transfected with CLIC5A cDNA or vector alone. Data show the mean±s.e.m. (n=3 independent experiments); *P=0.005 (Student's t-test). (C) CLIC5A (rabbit anti-CLIC5A) and phospho-ERM (mouse anti-phospho-Thr567 ezrin) immunoreactivity (upper panel) and GFP–CLIC5A fluorescence and phospho-ERM (rabbit anti-phospho-Thr567 ezrin) immunoreactivity (lower panel) were detected by confocal immunofluorescence microscopy (image acquisition at 40× magnification) in TCA-fixed COS-7 cells transiently transfected 48 h prior to fixation with cDNA encoding CLIC5A or GFP–CLIC5A. Arrows indicate CLIC5A-transfected cells. Untransfected cells in the monolayer (*) served as controls. Scale bar: 10 μm.

Journal of Cell Science (2014) 127, 5164–5178 doi:10.1242/jcs.147744

cells expressing CLIC5A than in those of vector-transfected cells (Fig. 1A, Lysate). Two phospho-ERM protein bands corresponding to phospho-ezrin and phospho-moesin, based on their respective molecular mass, were observed in COS-7 cells and both were hyperphosphorylated in the presence of CLIC5A. Densitometric quantification showed that the ratio of phospho-ERM to total ezrin increased approximately threefold when COS-7 cells expressed ectopic CLIC5A, relative to vector-transfected cells (Fig. 1B, Lysate).

Given that phosphorylated ERM proteins associate with F-actin (Bretscher et al., 2002; Ivetic and Ridley, 2004), we determined whether ectopic CLIC5A expression alters the association of ezrin with the cytoskeletal fraction. Cytoskeletons were prepared by lysing adherent cells with Triton X-100 and then harvesting the detergent-insoluble material that remained attached to the plates (Berryman et al., 2004). The amount of total ezrin and phospho-ERM associated with such cytoskeletal preparations was much greater in CLIC5A-transfected than in vector-transfected cells (Fig. 1A, Cytoskeleton). Densitometric quantification showed that at least sixfold more phospho-ERM was associated with the cytoskeleton of cells expressing CLIC5A compared with that of cells transfected with vector alone (Fig. 1B, Cytoskeleton). Overexposure might have led to underestimation of phospho-ERM abundance in the cytoskeletons. There also was approximately fourfold more total ezrin and phospho-ERM in Triton-X-100-insoluble fractions prepared from whole CLIC5A-transfected COS-7 cells than in similar fractions prepared from cells transfected with vector alone (data not shown). Because total ezrin abundance in whole SDS lysates was unchanged when CLIC5A was expressed (Fig. 1A), the results indicate that a greater fraction of ezrin is phosphorylated and therefore associates with the cytoskeleton when CLIC5A is expressed.

Confocal immunofluorescence microscopy also showed that phospho-ERM immunofluorescence was greater in COS-7 cells transfected with CLIC5A or GFP–CLIC5A compared with that in cells that remained untransfected (Fig. 1C). Hence, ectopic CLIC5A expression in COS-7 cells results in enhanced ERM phosphorylation.

Actin polymerization and cell surface remodeling in CLIC5A-transfected COS-7 cells

It is well established that ezrin phosphorylation can induce the formation of actin-rich apical protrusions (Yonemura et al., 1999; Zwaenepoel et al., 2012). We therefore determined whether ectopic CLIC5A expression in COS-7 cells altered actin polymerization and cell surface architecture. COS-7 cells were co-transfected with CLIC5A and YFP–actin or with vector and YFP–actin, both at a 10:1 (CLIC5A or vector:YFP–actin) ratio to maximize the probability of co-transfection of CLIC5A and vector with the reporter, and evaluated 48 h later by confocal microscopy. Substantially more YFP–actin organized in filaments was observed in cells that were (presumably) transfected with CLIC5A than in vector-transfected cells (Fig. 2A). By using scanning electron microscopy (SEM), we observed that many cells displayed cell surface projections and ruffles in cultures transfected with CLIC5A. Such projections were not observed in cultures of vector-transfected cells (Fig. 2B). Rhodamine–phalloidin staining also revealed an increase in polymerized actin in CLIC5A-transfected compared with vector-transfected cells (Fig. 2C). These data indicate that CLIC5A increases actin polymerization and cell surface remodeling, consistent with previous reports for CLIC5A (Berryman et al., 2004) and CLIC4 (Viswanatha et al., 2013).

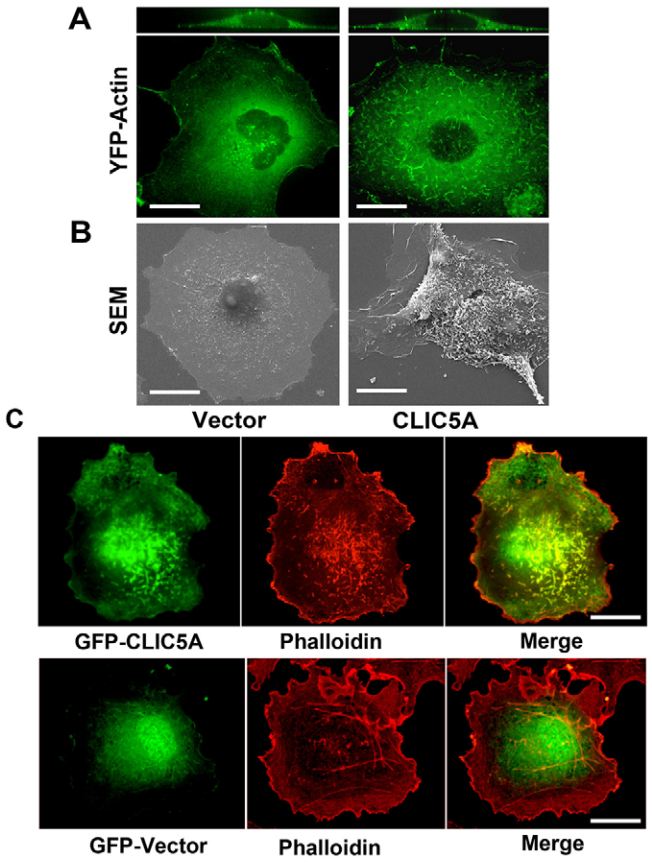

Fig. 2. Ectopic CLIC5A expression alters the cell surface architecture of COS-7 cells. (A) CLIC5A induces YFP–actin assembly. COS-7 cells were co-transfected with YFP–actin and CLIC5A or vector alone at a 1:10 ratio (YFP–actin:CLIC5A or vector) to maximize the probability that YFP–actin-transfected cells are also CLIC5A transfected. YFP was visualized by live-cell confocal immunofluorescence microscopy. (B) CLIC5A induces the formation of surface projections and ruffles in COS-7 cells. COS-7 cells were transfected with CLIC5A or vector followed by glutaraldehyde fixation, processing and SEM 48 h later. Because cells with surface ruffles were only observed in cultures that had been transfected with CLIC5A, it is assumed that ruffled cells were CLIC5A transfected. (C) Detection of polymerized actin with Rhodamine–phalloidin in COS-7 cells transfected with GFP–CLIC5A or GFP alone. Cells were fixed with 4% paraformaldehyde and labeled with Rhodamine–phalloidin and rabbit anti-CLIC5A antibody. Actin-containing ruffles in which phalloidin and CLIC5A colocalized were observed in the CLIC5A-transfected cells. Scale bars: 10 μm.

CLIC5A does not inhibit ERM phosphatases

We next examined whether the increase in ERM phosphorylation in response to CLIC5A could reflect the inhibition of ERM phosphatases. It was reported previously that both PKC and ROCK can phosphorylate ERM proteins on the conserved C-terminal Thr residue (Ivetic and Ridley, 2004). Untransfected COS-7 cells were therefore treated with the PKC inhibitor staurosporine (SSP), the ROCK inhibitor Y27632 and the protein phosphatase 1 inhibitor calyculin A (Cal-A). In the presence of Cal-A, phospho-ERM abundance increased substantially in SDS-soluble COS-7 cell lysates, indicating that Cal-A-sensitive phosphatases actively dephosphorylate ERM proteins in COS-7 cells. Conversely, SSP treatment significantly reduced ERM phosphorylation, whereas Y27632 was essentially without effect (Fig. 3A, Lysate). Thus, PKC is the principal kinase phosphorylating ERM proteins in COS-7

Journal of Cell Science (2014) 127, 5164–5178 doi:10.1242/jcs.147744

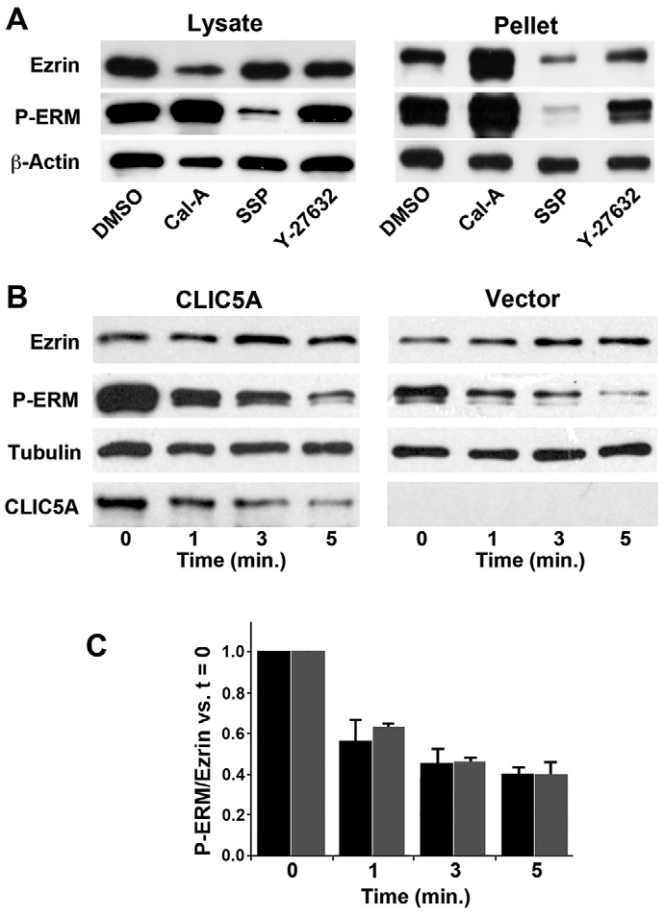

Fig. 3. CLIC5A does not inhibit P-ERM dephosphorylation. (A) Phosphorylation of ERM proteins in untransfected COS-7 cells is predominantly mediated by PKC. COS-7 cells were treated with the protein phosphatase 1 inhibitor calyculin A (Cal-A, 100 nM, 15 min), the PKC inhibitor staurosporine (SSP, 100 nM, 60 min), the ROCK inhibitor Y-27632 (15 μM, 60 min) or vehicle (DMSO, 60 min) followed by western blot analysis of phospho-ERM (P-ERM; mouse anti-phospho-Thr567 ezrin) and total ezrin (rabbit anti-ezrin) in SDS-solubilized cells (Lysate) and in the Triton-X-100-insoluble cytoskeletal fraction (Pellet). β-actin (mouse anti-β-actin) served as the loading control and rabbit anti-CLIC5A was used to verify CLIC5A protein expression. Phospho-ERM abundance and cytoskeleton-associated ezrin increased in response to Cal-A. Staurosporine, but not Y-27632, inhibited ERM phosphorylation and ezrin association with the cytoskeleton. (B,C) CLIC5A does not block the dephosphorylation of phospho-ERM proteins. (B) Western blot analysis of COS-7 cell lysates transiently transfected with CLIC5A cDNA or vector and treated with staurosporine (100 nM) for 1, 3 or 5 min. Control cells (t=0) were not treated with staurosporine. The blots were probed with rabbit anti-ezrin, mouse anti-phospho-Thr567 ezrin, rabbit anti-CLIC5A and mouse anti-tubulin antibodies. (C) Densitometric analysis [mean phospho-ERM:ezrin ratio relative to t=0 (±s.e.m.), three independent experiments]. Although phospho-ERM was greater at t=0 in CLIC5A- than in vector-transfected cells (B), the rate of phospho-ERM dephosphorylation was similar in CLIC5A- (black bars) and vector-transfected cells (grey bars).

cells. In keeping with the findings in cell lysates, Cal-A enhanced and SSP strongly reduced the amount of ezrin and phospho-ERM in Triton-X-100-resistant cytoskeletal fractions (Fig. 3A).

To determine whether CLIC5A blocks ERM phosphatases, we evaluated the rate of ERM dephosphorylation during PKC inhibition. Although the amount of phospho-ERM was again much greater in CLIC5A-transfected compared with vector-transfected cells, the abundance of phospho-ERM declined rapidly upon addition of SSP in both CLIC5A- and vector-transfected cells, without any change in total ezrin abundance (Fig. 3B). Nonetheless, the rate at which the phospho-ERM:total ezrin ratio declined did not differ between COS-7 cells expressing CLIC5A and those transfected with the vector alone (Fig. 3C). These findings suggest that the increase in ERM phosphorylation in cells expressing CLIC5A cannot be attributed to inhibition of ERM phosphatase(s). Interestingly, the abundance of the CLIC5A immunoreactive band also declined rapidly upon SSP addition. This finding implies either that CLIC5A is rapidly degraded or that it undergoes a conformational change and reduced antibody reactivity upon PKC inhibition.

The effect of CLIC5A on plasma membrane charge distribution and PI(4,5)P_2 abundance

We next determined whether ectopic expression of CLIC5A alters the negative surface potential of the plasma membrane inner leaflet in COS-7 cells by co-transfecting them with the surface potential reporter GFP–Kras (Yeung et al., 2006) and CLIC5A or empty vector. Live-cell imaging revealed that the surface potential biosensor GFP–Kras was evenly distributed along the plasma membrane in the absence of CLIC5A. There was a dramatic redistribution of GFP–Kras into plasma membrane clusters at the cell surface in the presence of CLIC5A (Fig. 4A). The head of PI(4,5)P_2 is negatively charged, and PI(4,5)P_2 is required as a membrane anchor for ERM protein activation and phosphorylation (Fievet et al., 2004). We therefore investigated whether CLIC5A alters the distribution of PI(4,5)P_2 in COS-7 cells, by co-transfecting them with the PI(4,5)P_2 biosensor GFP–PH-PLC and CLIC5A or vector alone. To maximize co-transfection, the ratio of GFP–PH-PLC reporter:CLIC5A or vector cDNA was 1:10. Live-cell imaging showed that the PI(4,5)P_2 reporter localized to plasma membrane clusters that extended vertically from the COS-7 cell surface (Fig. 4B), and that these sites of PI(4,5)P_2 accumulation were more abundant in CLIC5A-transfected than in vector-transfected cells. The dorsal membrane:cytoplasm GFP–PH-PLC ratio was significantly greater in CLIC5A-transfected than in vector-transfected cells, indicating an increase in dorsal plasma membrane PI(4,5)P_2 abundance in CLIC5A-expressing cells (Fig. 4C).

When COS-7 cells were co-transfected with RFP–PH-PLC and GFP–CLIC5A (ratio 1:10), there was substantial colocalization of GFP–CLIC5A with the PI(4,5)P_2 reporter at the dorsal plasma membrane (Fig. 4D, X-*Z*). In control cells, GFP remained cytoplasmic and did not colocalize with the PI(4,5)P_2 reporter. Examination of *Z*-stacks revealed that the PI(4,5)P_2 reporter was organized in surface ruffles whose density was much greater in cells transfected with CLIC5A compared with that of vector-transfected cells (Fig. 4D). These experiments suggest strongly that the reorganization of the dorsal plasma membrane in COS-7 cells transfected with CLIC5A is accompanied by a polarized accumulation of PI(4,5)P_2 in cell surface clusters containing CLIC5A.

PLC activation blocks CLIC5A-dependent ERM phosphorylation

PI(4,5)P_2 is a substrate for PLC, and substantial PLC activation depletes plasma membrane PI(4,5)P_2. We therefore determined whether activation of PLC would alter CLIC5A-induced ERM phosphorylation. COS-7 cells transfected with CLIC5A or vector alone were treated with 800 μM of the PLC activator m-3M3FBS. As early as 5 min after initiation of m-3M3FBS treatment, ERM phosphorylation decreased significantly in both CLIC5A- and vector-transfected cells (Fig. 5A), and the effect of CLIC5A on

Journal of Cell Science (2014) 127, 5164–5178 doi:10.1242/jcs.147744

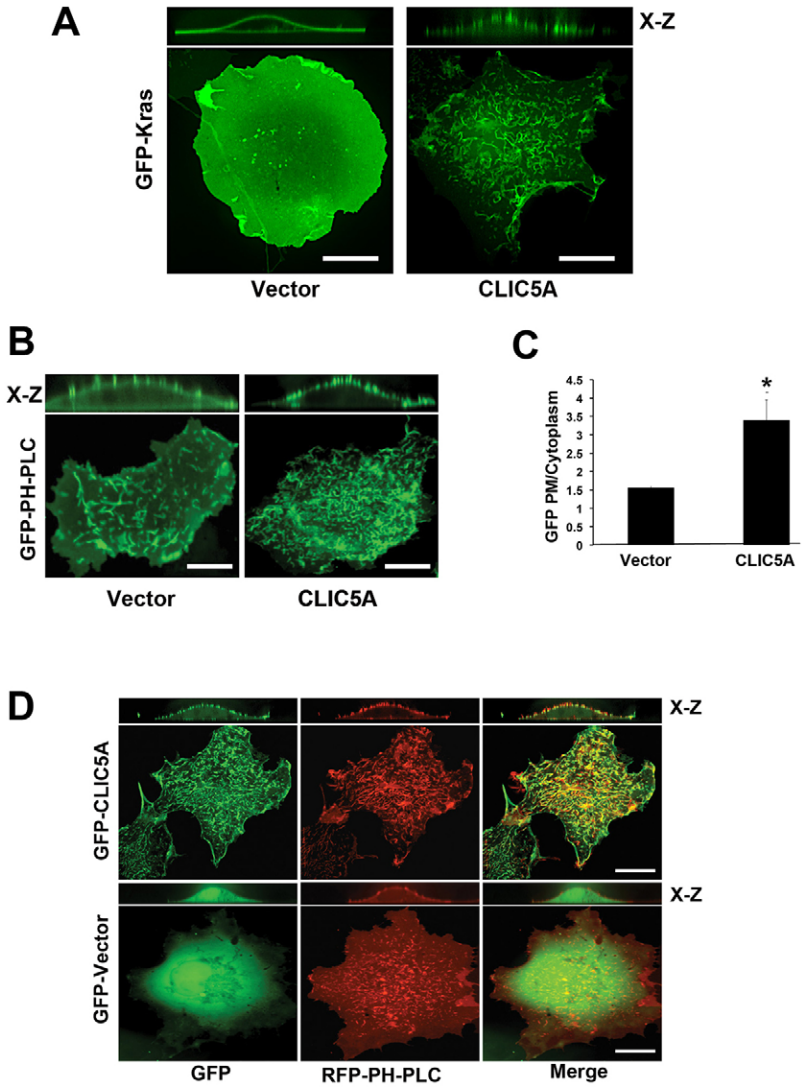

Fig. 4. Clustered dorsal PI(4,5)P_2 accumulation in the presence of CLIC5A. (A) CLIC5A-dependent redistribution of plasma membrane negative surface potential. COS-7 cells were co-transfected with the surface potential biosensor GFP–Kras and CLIC5A cDNA or vector (10:1, CLIC5A or vector:GFP–Kras). GFP–Kras was visualized with spinning-disk confocal microscopy in living cells 48 h later. In vector-transfected cells, GFP–Kras was distributed uniformly along dorsal and basal cell membranes. In CLIC5A-transfected cells, GFP–Kras was concentrated in dorsal plasma membrane clusters that appeared to project from the cell surface in the stacked image. Scale bar: 10 μm. (B) CLIC5A-dependent accumulation of PI(4,5)P_2 in the dorsal plasma membrane. COS-7 cells were co-transfected with CLIC5A cDNA or vector and the PI(4,5)P_2 biosensor GFP–PH-PLC (ratio 10:1, CLIC5A or vector:GFP–PH-PLC), followed 48 h later by spinning-disk confocal microscopy in living cells. In vector-transfected cells, clusters of GFP–PH-PLC at the dorsal cell membrane and diffuse GFP fluorescence in the cytoplasm are observed. In CLIC5A-transfected cells, significantly more GFP–PH-PLC is observed in dorsal membrane clusters than in vector-transfected cells, and cytoplasmic GFP fluorescence is reduced. Scale bar: 10 μm. (C) The ratio of dorsal membrane:cytoplasmic GFP–PH-PLC fluorescence is significantly greater in CLIC5A- than in vector-transfected cells. PM, plasma membrane. Data show the mean±s.e.m. (n=10 cells per experiment, three independent experiments); *P<0.01 (Student's t-test). (D) Colocalization of the PI(4,5)P_2 biosensor RFP–PH-PLC with GFP–CLIC5A. COS-7 cells were co-transfected with the PI(4,5)P_2 biosensor RFP–PH-PLC and GFP–CLIC5A (upper panels) or GFP (lower panels) (ratio 10:1, CLIC5A or GFP:RFP–PH-PLC). GFP and RFP were visualized by spinning-disk confocal microscopy in living cells. The RFP–PH-PLC colocalized with GFP–CLIC5A, but not GFP, at the dorsal plasma membrane (*X-Z*). Scale bar: 10 μm.

ERM phosphorylation was lost. In HeLa cells transfected with CLIC5A or vector and then treated with m-3M3FBS, CLIC5A-dependent ERM phosphorylation was similarly lost (data not shown). The abundance of CLIC5A also declined in response to m-3M3FBS (Fig. 5A). Imaging revealed that dorsal plasma membrane clusters bearing the RFP–PH-PLC reporter were reduced in a time-dependent fashion after m-3M3FBS treatment, and CLIC5A was redistributed into the cytosol (Fig. 5B). These findings suggest that CLIC5A-dependent ERM phosphorylation is abrogated in response to PI(4,5)P_2 depletion, and are consistent with the possibility that the alteration in the distribution of GFP–Kras (Fig. 4A) and GFP–PH-PLC or RFP–PH-PLC (Fig. 4B,D) in CLIC5A-transfected cells results from changes in PI(4,5)P_2 abundance in the dorsal plasma membrane. The finding that m-3M3FBS also reduced CLIC5A association with the dorsal plasma membrane and resulted in a reduction in CLIC5A abundance suggests that the association of CLIC5A with the dorsal plasma membrane of cells is itself dependent on PI(4,5)P_2.

CLIC5A-mediated ERM phosphorylation is not inhibited by IAA-94

Given that the ion conductance of CLIC5A is inhibited by IAA-94 (Berryman et al., 2004), we next determined whether IAA-94 alters ERM phosphorylation in COS-7 cells expressing CLIC5A. IAA-94 did not inhibit the increase in phospho-ERM abundance in cell lysates or in cytoskeletal fractions of COS-7 cells expressing CLIC5A (Fig. 5C). This observation suggests that the CLIC5A-dependent effect on ERM phosphorylation is independent of its putative ion channel activity.

CLIC5A colocalizes with PI4P5Kα at the dorsal plasma membrane and interacts with PI(4,5)P_2-generating kinases *in vitro*

The PI(4,5)P_2 in phospholipid bilayers is produced from phosphatidylinositol 4-phosphate (PI4P) by PI4P5 kinases, and to a lesser extent from phosphatidylinositol 5-phosphate (PI5P) by PI5P4 kinases (Divecha, 2010). All isoforms of these PI(4,5)P_2-generating kinases contain surface cationic residues conferring a positive charge that allows them to bind to negatively charged membrane phospholipids (Fairn et al., 2009). We therefore determined whether the presence of CLIC5A alters the distribution of PI4P5Kα in COS-7 cells. To this end, COS-7 cells were co-transfected with HA–PI4P5Kα and GFP–CLIC5A or GFP. There was considerable colocalization of GFP–CLIC5A with HA–PI4P5Kα at the dorsal plasma membrane (Fig. 6A, X-*Z*) but not with GFP in control cells.

To further probe whether CLIC5A might interact with PI(4,5)P_2-generating kinases, COS-7 cells were transfected with

Journal of Cell Science (2014) 127, 5164–5178 doi:10.1242/jcs.147744

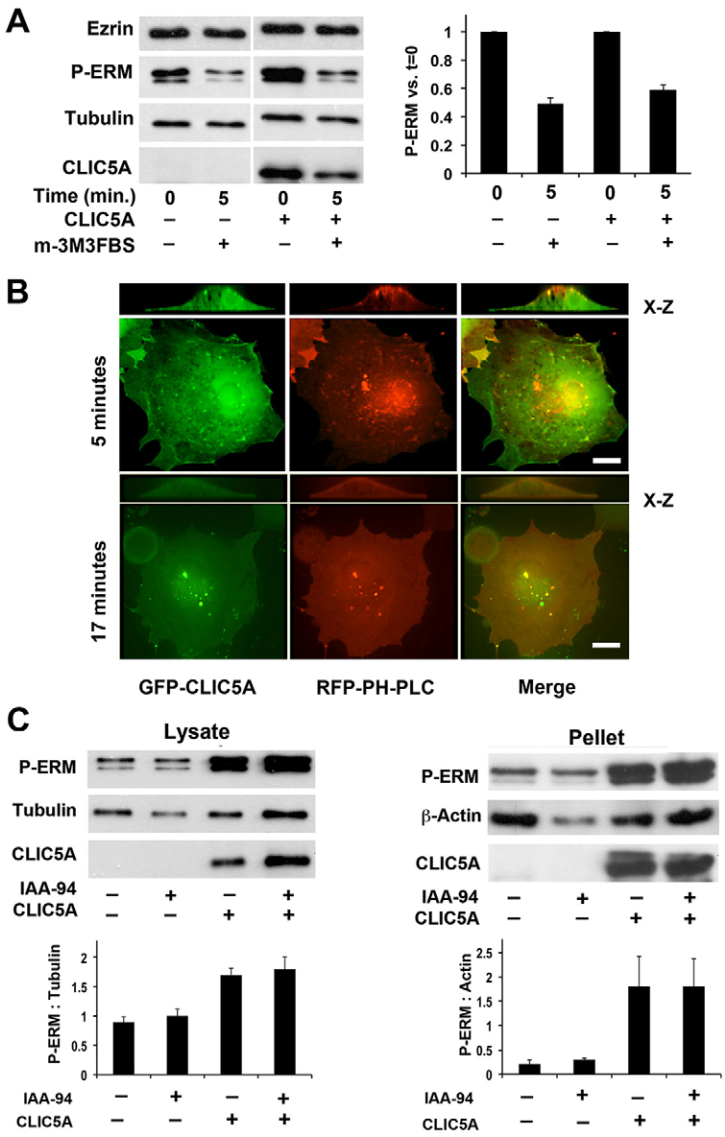

Fig. 5. Abrogation of CLIC5A-dependent ERM phosphorylation by m-3M3FBS, but not IAA-94. (A) PLC activation by m-3M3FBS inhibits ERM phosphorylation. Western blots and densitometric quantification (n=3 independent experiments) of SDS-solubilized COS-7 cells transfected with CLIC5A cDNA or vector, and treated with the PLC activator m-3M3FBS (800 μM) for 5 min. The blots were probed with rabbit anti-ezrin, mouse anti-phospho-Thr567 ezrin, rabbit anti-CLIC5A and mouse anti-tubulin antibodies. Treatment with m-3M3FBS reduced ERM phosphorylation in CLIC5A- and vector-transfected cells. Densitometric analysis shows that the magnitude of the m-3M3FBS-mediated phospho-ERM (P-ERM) dephosphorylation is similar in the presence and absence of CLIC5A. Data show the mean±s.e.m. (B) Time-dependent loss of PI(4,5)P_2 clusters and CLIC5A from the dorsal plasma membrane in response to m-3M3FBS. COS-7 cells co-transfected with CLIC5A cDNA and RFP–PH-PLC (10:1, CLIC5A:RFP–PH-PLC) were treated with the PLC activator m-3M3FBS (800 μM) for 5–17 min, followed by spinning-disk confocal microscopy in living cells. A time-dependent loss of dorsal membrane CLIC5A or RFP-PH-PLC clusters was observed, and substantial CLIC5A was redistributed into the cytosol. Scale bar: 10 μm. (C) The Cl^- channel inhibitor IAA-94 does not alter CLIC5A-dependent ERM phosphorylation. COS-7 cells were transfected with CLIC5A or vector. After 48 h, cells were treated with IAA-94 (50 μM, 30 min). Blots were probed with rabbit anti-ezrin, mouse anti-phospho-Thr567 ezrin and rabbit anti-CLIC5A. To control for loading, mouse anti-tubulin antibodies were used for blots of SDS-soluble lysates and mouse anti-β-actin for blots of the Triton-X-100-insoluble fraction. Densitometric analysis of results from three independent experiments shows that IAA-94 (50 μM, 30 min) does not alter CLIC5A-dependent ERM phosphorylation or cytoskeleton association. Data show the mean±s.e.m.

HA-tagged PI4P5Kα, PI4P5Kβ, PI5P4Kα and PI5P4Kβ cDNA. Cell lysates were then incubated with recombinant GST–CLIC5A or GST immobilized on glutathione–Sepharose beads. Western blot analysis of the eluted proteins showed that HA–PI4P5Kα (Fig. 6B) and HA–PI5P4Kα (Fig. 6C) in cell lysates bound to GST-CLIC5A but not to GST. Identical results were obtained with HA–PI4P5Kβ and HA–PI5P4Kβ (data not shown).

Occasionally, overexpression of CLIC5A or the combination of CLIC5A and HA–PI4P5Kα resulted in the formation of very large vacuoles in COS-7 cells. Such vacuoles were not observed in vector-transfected cells. CLIC5A and HA–PI4P5Kα were found to colocalize to the membrane of such vacuoles (Fig. 6D). In vacuolated cells transfected only with CLIC5A, the PI(4,5)P_2 reporter GFP–PH-PLC also localized to the vacuolar membranes (Fig. 6E). These data also support the concept that CLIC5A colocalizes with HA–PI4P5Kα at sites of PI(4,5)P_2 production.

Silencing of endogenous PI4P5Kα reduces CLIC5A-stimulated ERM phosphorylation

To further probe the functional interaction between CLIC5A and PI4P5Kα, endogenous PI4P5Kα was depleted using specific small interfering (si)RNA. In both COS-7 and HeLa cells, PI4P5Kα-specific but not nonspecific siRNA inhibited PI4P5Kα protein expression (Fig. 7A). Silencing of PI4P5Kα abrogated the effect of CLIC5A overexpression on ERM phosphorylation in both COS-7 and HeLa cells (Fig. 7A), consistent with an essential role for PI4P5Kα in CLIC5A-dependent ERM phosphorylation.

CLIC5A N- and C-terminal deletions abrogate its membrane association and PI(4,5)P_2-dependent ezrin phosphorylation

We next determined whether CLIC5A N- or C-terminal deletions would alter the functional effect on ERM phosphorylation. CLIC5A in which the first β-pleated sheet alone (CLIC5A$^{22–251}$), the first β-pleated sheet and the putative membrane-spanning domain (CLIC5A$^{55–251}$) or only the N-terminal ninth α-helix (CLIC5A$^{1–232}$) were deleted were therefore expressed in COS-7 cells. In contrast to wild-type CLIC5A, none of the deletion mutants supported enhanced ERM phosphorylation in COS-7 cells (Fig. 7B). The mutant CLIC5A proteins also failed to associate with the plasma membrane, did not colocalize with HA–PI4P5Kα (Fig. 7C) and failed to induce plasma membrane PI(4,5)P_2 accumulation (Fig. 7D). The mutant CLIC5A proteins

Journal of Cell Science (2014) 127, 5164–5178 doi:10.1242/jcs.147744

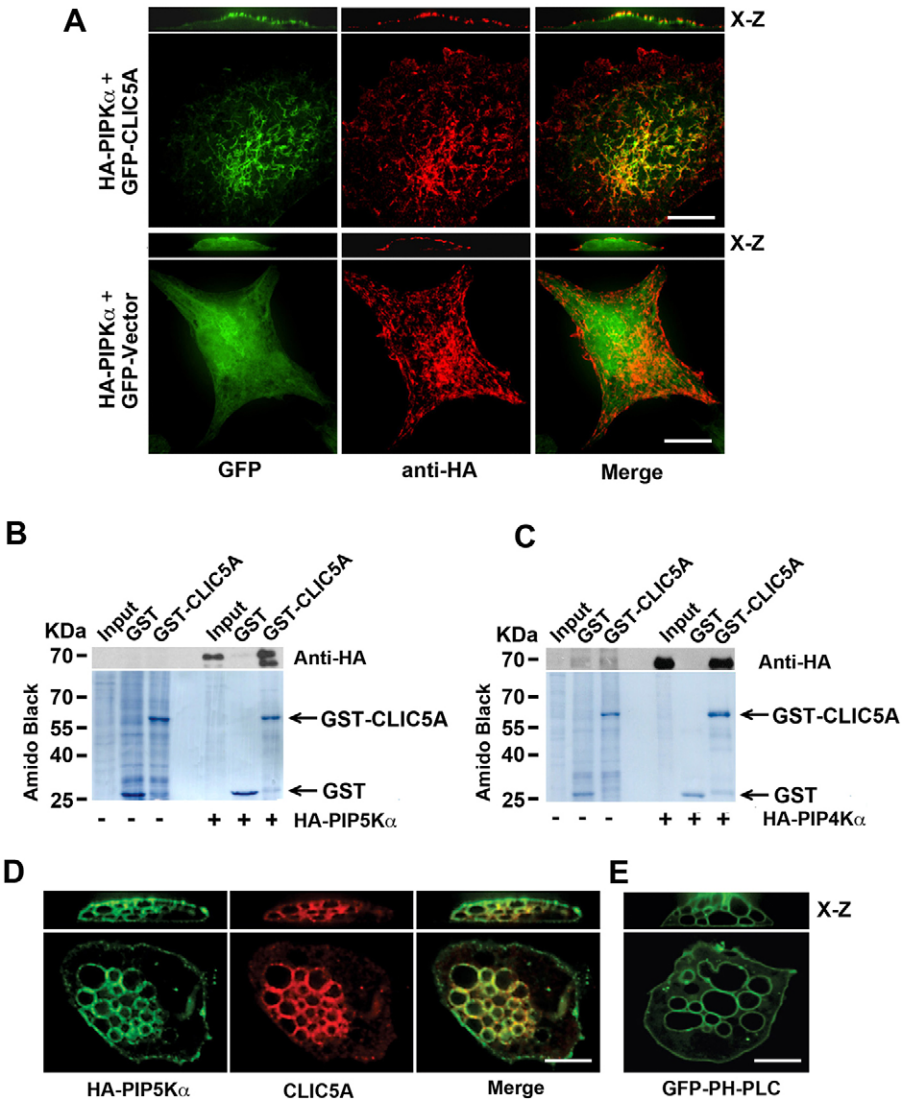

Fig. 6. Association of CLIC5A with PI4P5Kα. (A) CLIC5A colocalizes with PI4P5Kα. COS-7 cells were co-transfected with HA–PI4P5Kα and GFP–CLIC5A or GFP. Cells were fixed with 4% paraformaldehyde. GFP–CLIC5A and PI4P5Kα were detected by natural GFP fluorescence and rat anti-HA immunofluorescence, respectively. Considerable colocalization of GFP and HA–PIP5Kα is observed at the dorsal plasma membrane (*X-Z*) and in cellular ruffles (stacked image) of GFP–CLIC5A-transfected (upper panel), but not GFP-transfected cells (lower panel). Scale bar: 10 μm. (B,C) PI(4,5)P_2-generating enzymes associate with CLIC5A. Total cell lysates were prepared from COS-7 cells that had been transfected with HA–PI4P5Kα (B), HA–PI4P5Kβ (not shown), HA–PI5P4Kα (C) and HA–PI5P4Kβ (not shown). Cell lysates prepared with Triton X-100 lysis buffer were incubated with recombinant GST or GST–CLIC5A immobilized on glutathione–Sepharose beads. The beads were precipitated and washed exhaustively, and bound proteins were eluted and evaluated by western blot analysis. Lysate served as the 'input' control for each transfection and Amido Black staining of the membranes shows total (Input) and eluted proteins (GST, GST–CLIC5A). HA–PI4PK5α (B), HA–PI4P5Kβ (not shown), HA–PI5P4Kα (C) and HA–PI5P4Kβ (not shown) were all precipitated with immobilized GST–CLIC5A but not with GST. (D) Colocalization of CLIC5A and PI4P5Kα on vacuolar membranes. In cultures of COS-7 cells transfected with full-length wild-type CLIC5A and HA–PI4P5Kα, occasional cells developed large intracellular vacuoles. Cells were fixed with 4% paraformaldehyde. HA–PI4P5Kα (rat anti-HA) and CLIC5A (rabbit anti-CLIC5A) colocalized on the vacuolar membranes in such cells. Vacuoles were not observed in vector-transfected cells. (E) Confocal microscopy of living COS-7 cells co-transfected with wild-type CLIC5A cDNA and the PI(4,5)P_2 biosensor GFP–PH-PLC (1:10, CLIC5A cDNA:GFP–PH-PLC cDNA). In cells that developed large vacuoles after transfection with wild-type CLIC5A, the PI(4,5)P_2 reporter also localized to the vacuolar membranes, even in the absence of HA–PI4P5Kα. Scale bars: 10 μm (D,E).

did not achieve the level of expression obtained for full-length CLIC5A (Fig. 7B), leaving open the possibility that the functional defect is related, in part, to low levels of expression. Nonetheless, the findings suggest that both N- and C-termini are required for the membrane association of CLIC5A, and potentially also for the stabilization of CLIC5A in the plasma membrane. Although the dorsal plasma membrane localization of PI4P5Kα appears to be independent of CLIC5A, increased PI(4,5)P_2 accumulation was nonetheless dependent on the presence of full-length CLIC5A. This finding implies that CLIC5A is not required for the recruitment of PI4P5Kα to the plasma membrane, but that it is required for localized PI4P5 and/or PI5P4 kinase activation.

The absence of CLIC5A *in vivo* is associated with reduced ezrin function in renal glomeruli

CLIC5A is expressed at extraordinarily high levels in renal glomeruli (Nyström et al., 2009), where it colocalizes with ezrin

Journal of Cell Science (2014) 127, 5164–5178 doi:10.1242/jcs.147744

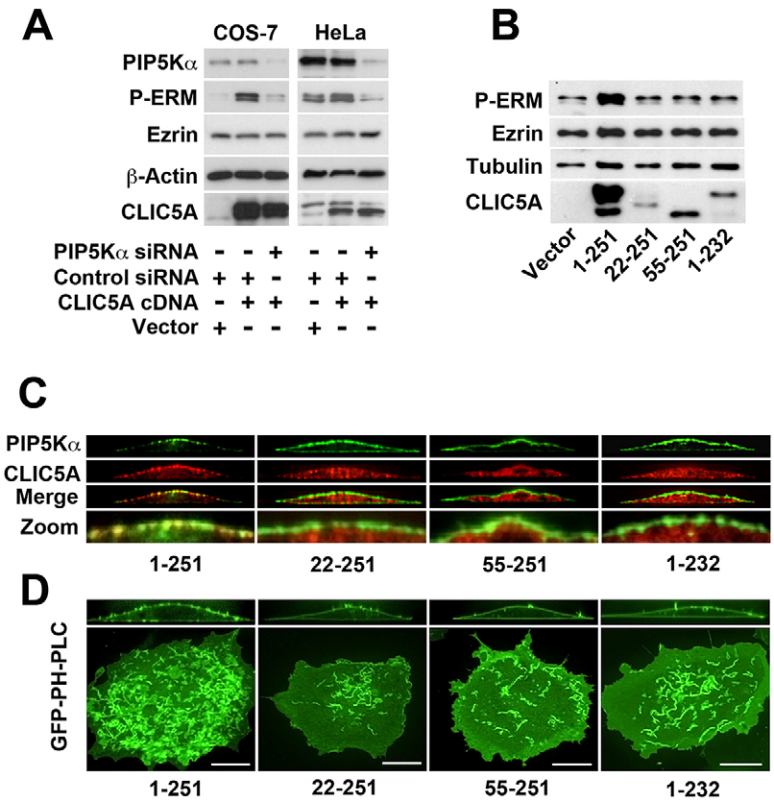

Fig. 7. The effect of CLIC5A on ERM phosphorylation is abrogated by PI4P5Kα silencing and by disruption of CLIC5A membrane association. (A) Silencing of endogenous PI4P5Kα blocks CLIC5A-dependent ERM phosphorylation. COS-7 or HeLa cells were co-transfected with CLIC5A cDNA or vector and control or PI4P5Kα-specific siRNA. Whole-cell lysates were evaluated for PI4P5Kα, phospho-ERM (P-ERM), ezrin, β-actin and CLIC5A protein abundance by western blot analysis. (B) CLIC5A mutants fail to augment ERM phosphorylation. COS-7 cells were co-transfected with HA–PI4P5Kα and full-length wild-type CLIC5A (1–251) or CLIC5A mutants in which the first β-pleated sheet (22–251), the first β-pleated sheet and the putative transmembrane domain (55–251) or the ninth α-helical domain (1–232) had been deleted, followed by western blot analysis of SDS-solubilized COS-7 cells at 48 h after transfection. The blots were probed with rabbit anti-ezrin, mouse anti-phospho-Thr567 ezrin, rabbit anti-CLIC5A and mouse anti-tubulin antibodies. Full-length CLIC5A induced ERM phosphorylation, but the CLIC5A deletion mutants did not. (C) CLIC5A mutants do not associate with the dorsal plasma membrane. COS-7 cells were co-transfected with HA–PI4P5Kα and full-length wild-type CLIC5A (1–251) or CLIC5A mutants as in B, followed 48 h later by fixation with 4% paraformaldehyde and dual-label confocal immunofluorescence analysis for PI4P5Kα (rat anti-HA) and CLIC5A (rabbit anti-CLIC5A). Full-length wild-type CLIC5A localized to the plasma membrane and co-localized partially with HA–PI4P5Kα. The CLIC5A mutants failed to localize to the plasma membrane and did not colocalize with HA–PI4P5Kα. (D) CLIC5A mutants do not increase dorsal PI(4,5)P_2 accumulation. COS-7 cells were co-transfected with GFP–PH-PLC and wild-type CLIC5A or CLIC5A mutants as in A (10:1, CLIC5A cDNA:GFP–PH-PLC cDNA), followed by evaluation of living cells for GFP fluorescence with confocal microscopy. Substantially more PI(4,5)P_2 reporter localized to the dorsal plasma membrane in cells transfected with full-length wild-type CLIC5A than in cells transfected with CLIC5A mutants. Scale bars: 10 μm.

in podocytes (Pierchala et al., 2010; Wegner et al., 2010). In turn, ezrin interacts with the transmembrane protein podocalyxin (Orlando et al., 2001), with NHERF2 as the intermediary (Takeda, 2003). We now observe that much less ezrin and phospho-ERM are associated with the detergent-insoluble fraction of glomeruli from CLIC5-deficient mice compared with wild-type mice (Fig. 8A). In glomerular podocytes, phospho-ezrin binds to NHERF2, coupling it to the cytoskeleton. We therefore determined whether deletion of CLIC5A would also alter the association of NHERF2 with the cytoskeletal fraction. Because NHERF2 is expressed predominantly in glomeruli (Wade et al., 2001), kidney cortex was used for these experiments. Substantial NHERF2 was observed in the detergent-insoluble fraction of kidney cortex lysate from wild-type mice, but in CLIC5-deficient mice most of the NHERF2 remained associated with the detergent-soluble fraction (Fig. 8B). Furthermore, the colocalization of phospho-ERM with podocalyxin observed in wild-type mice was markedly reduced in the glomeruli of CLIC5-deficient mice (Fig. 8C). Thus, CLIC5A also regulates ERM phosphorylation and function *in vivo*, in keeping with the increased susceptibility to glomerular injury in these mice (Wegner et al., 2010).

DISCUSSION

CLIC and ERM proteins are commonly associated (Jiang et al., 2014), and both CLIC5A and CLIC4 have been shown previously to associate with ezrin and to induce cell surface microvillus formation in epithelial cells (Berryman et al., 2004; Viswanatha et al., 2013). However, the mechanism(s) governing the functional interactions between CLICs and ERM proteins are not understood. Here, we focused on CLIC5A, which is associated with radixin in sensory stereocilia of inner ear hair cells (Gagnon et al., 2006; Salles et al., 2013) and with ezrin in renal glomerular podocytes (Wegner et al., 2010). We observe that ectopic CLIC5A expression in COS-7 cells, which are null for CLIC5A at baseline, strongly stimulates ERM phosphorylation, ezrin association with the cytoskeleton and remodeling of the dorsal membrane architecture. CLIC5A

Journal of Cell Science (2014) 127, 5164–5178 doi:10.1242/jcs.147744

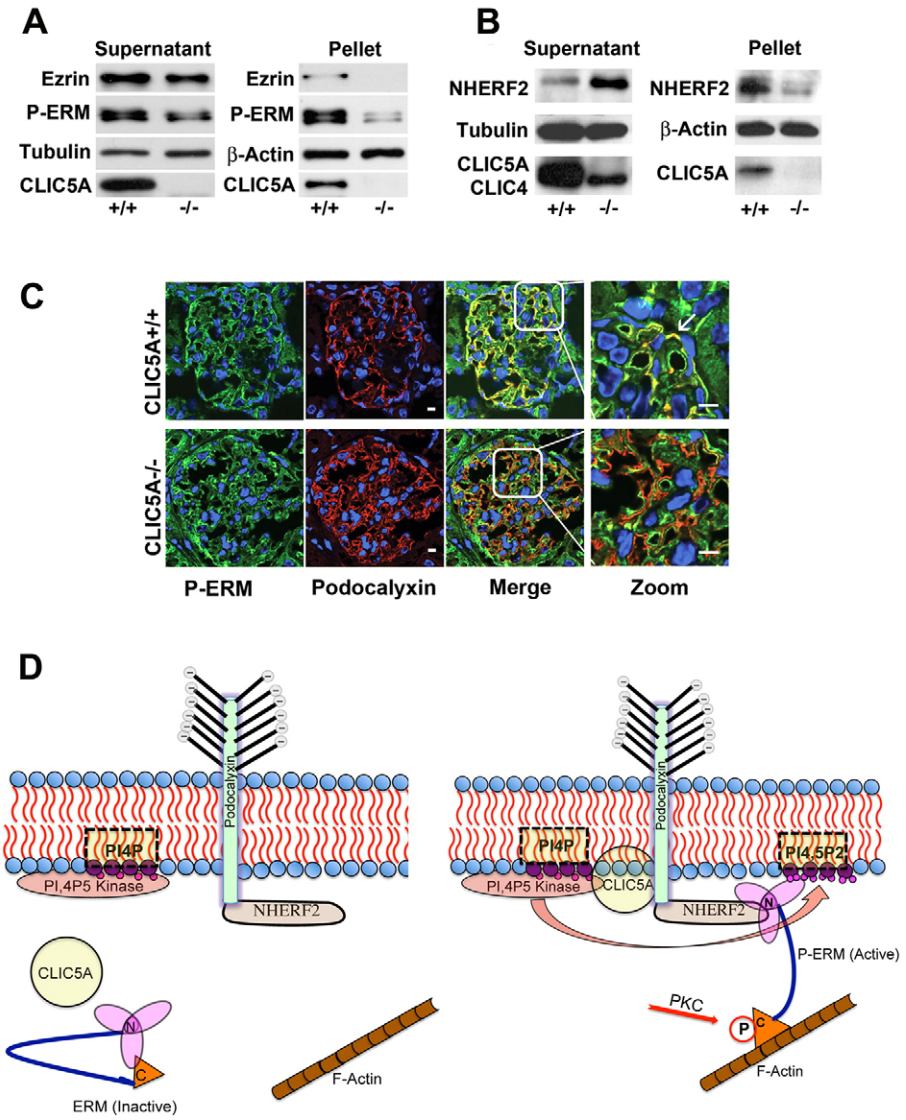

Fig. 8. CLIC5 deletion reduces ezrin phosphorylation in renal glomeruli and disrupts the ezrin–NHERF2–podocalyxin complex. (A) Glomeruli were isolated from wild-type (+/+) and CLIC5-deficient (−/−) mice. Whole glomeruli were solubilized in Nonidet P40/deoxycholate lysis buffer followed by sedimentation of the detergent-insoluble fraction. Detergent-soluble (Supernatant) and detergent-insoluble (Pellet) fractions were then evaluated by western blot analysis using rabbit anti-CLIC5A, rabbit anti-ezrin and mouse anti-phospho-Thr567 ezrin antibodies. Mouse anti-tubulin was used as the loading control for the supernatants and mouse anti-β-actin for the pellet. CLIC5A was observed in lysates and pellets from wild-type but not CLIC5-deficient mice. The phospho-ERM (P-ERM) abundance was reduced in the detergent-soluble fraction from glomeruli of CLIC5-deficient mice, consistent with previous findings (Wegner et al., 2010). Much less ezrin was observed in the detergent-insoluble fraction of glomeruli from CLIC5-deficient mice compared with that of wild-type mice. (B) Renal cortex from wild-type and CLIC5-deficient mice was homogenized in Nonidet P40/deoxycholate lysis buffer and then separated into soluble (Supernatant) and insoluble (Pellet) fractions followed by western blot analysis. In wild-type mice, substantial NHERF2 was observed in the pellet, whereas NHERF2 remained soluble in CLIC5-deficient mice. (C) Confocal immunofluorescence microscopy for phospho-ERM (rabbit anti-phospho-Thr567 ezrin) and podocalyxin (goat anti-podocalyxin) in TCA-fixed renal glomeruli from wild-type and CLIC5-deficient mice. Nuclei (blue) were visualized with DAPI (4′,6-Diamidino-2-Phenylindole). Phospho-ERM is present in glomeruli of both wild-type and CLIC5-deficient mice, but colocalization of phospho-ERM with podocalyxin was substantially reduced in CLIC5-deficient mice compared with that observed in wild-type mice. Scale bar: 10 μm. (D) Schematic model of CLIC5A function in glomerular podocytes. It is postulated that the association of CLIC5A with the inner leaflet of the dorsal plasma membrane serves to promote the generation of clustered $PI(4,5)P_2$. Ezrin binding to $PI(4,5)P_2$ in turn frees the ezrin C-terminus to bind to actin and to promote PKC-dependent ezrin phosphorylation. In the presence of CLIC5A, the active form of ezrin couples the intracellular tail of podocalyxin to actin, a key determinant of the normal apical podocyte architecture.

induces highly localized $PI(4,5)P_2$ accumulation in discrete clusters at the dorsal plasma membrane and colocalizes with overexpressed HA–PI4P5Kα in these clusters. Furthermore, GST–CLIC5A can pull down several $PI(4,5)P_2$-generating kinases from cell lysates, and PLC activation, which depletes $PI(4,5)P_2$, brings CLIC5A-dependent ezrin phosphorylation back to control levels as does silencing of endogenous PI4P5Kα expression. CLIC5A deletion mutants that fail to localize to the plasma membrane also fail to support clustered $PI(4,5)P_2$ accumulation and ERM phosphorylation. The data suggest that CLIC5A serves to increase $PI(4,5)P_2$ formation in discrete dorsal plasma membrane clusters to promote localized ERM phosphorylation, which in turn supports the formation of cell surface projections. Because the effect of CLIC5A is crucially

Journal of Cell Science (2014) 127, 5164–5178 doi:10.1242/jcs.147744

dependent on its association with the plasma membrane, we postulate that CLIC5A might be essential for the formation of a signaling complex that leads to the activation of $PI(4,5)P_2$-generating kinases specifically targeting localized ERM activation. The findings in renal glomeruli, where deletion of CLIC5A leads to reduced ERM phosphorylation and function are consistent with a similar role for CLIC5A in ERM phosphorylation *in vivo*.

The hypothesis that CLIC5A regulates ERM phosphorylation was based on previous findings that CLIC5A is associated with ERM proteins in sensory stereocilia and podocyte foot processes, and that ERM protein abundance is reduced in these locations in CLIC5-deficient mice (Gagnon et al., 2006; Wegner et al., 2010). Ezrin mRNA expression in the glomeruli of CLIC5-deficient mice is not reduced (A.A.-M., data not shown) and unphosphorylated ERM proteins are more readily degraded, which raised the possibility that CLIC5A might regulate ezrin phosphorylation. We found that ectopic expression of CLIC5A in COS-7 cells leads to a significant and highly reproducible increase in ERM phosphorylation and its association with the cytoskeletal fraction (Fig. 1). Nonetheless, in the COS-7 cells, overall ezrin abundance did not appear to change in the presence of CLIC5A. Therefore, whether the reduced ERM protein abundance in sensory stereocilia and podocytes of CLIC5-deficient mice results from ezrin destabilization due to reduced phosphorylation remains unclear.

The activity of ERM proteins involves phosphorylation-dephosphorylation cycles. Phosphorylation is stimulated by PKC, ROCK (Ivetic and Ridley, 2004) and AKT2 (Shiue et al., 2005), and dephosphorylation by myosin phosphatase and protein phosphatase 2C (PP2C) (Ivetic and Ridley, 2004). In COS-7 cells, inhibition of PKC but not ROCK inhibited ERM phosphorylation (Fig. 3), and we found no change in Thr308 and Ser473 phosphorylation of AKT2 in response to CLIC5A (data not shown). These results are consistent with the previous report showing no effect of the potent RhoA kinase inhibitor C3 transferase on ERM phosphorylation in various kidney-derived epithelial cells (Yonemura et al., 2002). Although ERM protein phosphorylation was much greater in the presence than in the absence of CLIC5A, the rate of ERM dephosphorylation during PKC inhibition was not altered by CLIC5A, suggesting that the effect of CLIC5A on ERM phosphorylation is not explained by inhibition of ERM phosphatases. Interestingly, we observed a consistent rapid decline in CLIC5A abundance upon treatment of COS-7 cells with SSP (Fig. 3B). The cause for the reduction in CLIC5A abundance is not yet clear, but given that SSP rapidly induces apoptosis in cells, it is conceivable that CLIC5A is subject to caspase-mediated cleavage. Alternatively, it is also possible that CLIC5A itself is phosphorylated by PKC and that inhibition of PKC induces a conformational change altering antibody reactivity. Further work will be needed to determine the mechanism whereby SSP causes the CLIC5A abundance to decline.

The CLIC proteins are redox sensitive and partition into lipid bilayers upon oxidation (Goodchild et al., 2009; Littler et al., 2005; Littler et al., 2004; Valenzuela et al., 2013), where they have ion-conducting properties that are blocked by IAA-94. Indeed, bovine CLIC5B (p64) was first isolated from kidney by affinity purification with IAA-94 (Landry et al., 1993; Redhead et al., 1992). It has been argued that CLICs might not function as Cl^- channels because the better characterized inhibitors SIDS or DIDS are without effect on CLIC ion conductance (Jentsch et al., 2002). However, in keeping with CLIC-mediated Cl^- ion conductance, a role in vacuolar and/or vesicular acidification has been reported for CLIC5B in osteoclasts (Edwards et al., 2006), for CLIC1 in macrophages (Jiang et al., 2012) and for CLIC4 in endothelial cells (Ulmasov et al., 2009). Here, we observed that the effect of CLIC5A on ERM phosphorylation was not inhibited by extracellular IAA-94 (Fig. 5C). It is possible that we did not achieve a sufficiently high intracellular concentration of IAA-94 to inhibit Cl^- conductance, but others have observed functional effects of IAA-94 in whole cells using the same concentration and timecourse (Orlando, 2002). It is also of note that CLIC5A expression leads to actin polymerization (Fig. 2A) and that F-actin inhibits CLIC-mediated ion conductance (Singh et al., 2007). Although our experiment does not exclude the possibility that CLIC5A forms ion-conducting pores when expressed in COS-7 cells, the data suggest that the effect of CLIC5A on ERM phosphorylation is not due an IAA-94-sensitive ion conductance.

Activation of ERM proteins requires the initial binding of the ERM N-terminus to $PI(4,5)P_2$, prompting a conformational change that then facilitates C-terminal actin binding and phosphorylation of a highly conserved threonine residue at the C-terminus (Bretscher et al., 2002; Ivetic and Ridley, 2004). $PI(4,5)P_2$ therefore plays an essential role in ERM phosphorylation (Barret et al., 2000; Niggli et al., 2001; Niggli et al., 1995). Because phospholipids are negatively charged, we first determined whether the presence of CLIC5A alters the plasma membrane negative charge distribution using the GFP–Kras reporter (Yeung et al., 2006). The dramatic clustering of the reporter at the dorsal plasma membrane of CLIC5A-transfected cells (Fig. 4A) could represent the remodeling of the dorsal plasma membrane (Fig. 2B), a redistribution of negatively charged lipids and/or binding of the reporter to the acidic foot loop (Cromer et al., 2007; Littler et al., 2010) of membrane-associated CLIC5A. Ectopic expression of CLIC5A was also associated with clustered accumulation of the $PI(4,5)P_2$ reporter GFP–PH-PLC at the dorsal plasma membrane of COS-7 cells, where it colocalized with CLIC5A (Fig. 4C). Redistribution of the $PI(4,5)P_2$ reporter from cytosol to plasma membrane (Fig. 4B) suggests enhanced $PI(4,5)P_2$ production at the plasma membrane in the presence of CLIC5A. It is conceivable that CLIC5A could functionally mimic $PI(4,5)P_2$, binding to the $PI(4,5)P_2$ reporter and directly supporting the conformational change in ezrin that then leads to its phosphorylation. Previous reports have shown that the PLC activator m-3M3FBS accelerates the hydrolysis of $PI(4,5)P_2$ and reduces the level of ERM phosphorylation in HeLa (Canals et al., 2012) and Jurkat T cells (Hao et al., 2009). In our studies, m-3M3FBS largely abolished increased ERM phosphorylation in the presence of CLIC5A. In addition, m-3M3FBS rapidly reduced the association of CLIC5A with the plasma membrane and immunoreactive CLIC5A in cell lysates. Hence, the finding that PLC activation abolished the effect of CLIC5A on ERM phosphorylation suggests that $PI(4,5)P_2$ mediates the effect of CLIC5A on ERM phosphorylation. The fact that CLIC5A redistributes to the cytosol upon PLC activation suggests that its association with the plasma membrane is also dependent on the plasma membrane phospholipid composition.

The PI4P5 kinases (PI4P5Kα, β and γ) phosphorylate the fifth position on the inositol ring of PI4P, producing the majority of $PI(4,5)P_2$ at the plasma membrane. The PI5P4 kinases also exist as α, β and γ isoforms and catalyze phosphorylation of the fourth

Journal of Cell Science (2014) 127, 5164–5178 doi:10.1242/jcs.147744

position on the inositol ring of PI5P to produce PI(4,5)P_2 (Rameh et al., 1997). It is already known that overexpression of PI4P5Kα induces actin polymerization (Shibasaki et al., 1997) and that all isoforms of PI4P5K contain a positively charged domain necessary for their recruitment to and association with negatively charged regions of the plasma membrane (Fairn et al., 2009). Indeed, recruitment of PI4P5 and/or PI5P4 kinases to the plasma membrane is necessary for PI(4,5)P_2 production. We observed that overexpressed HA–PI4P5Kα colocalizes with CLIC5A at the dorsal plasma membrane of COS-7 cells and that HA-tagged PI4P5K and PI5P4K α and β isoforms were pulled from cell lysates by GST–CLIC5A (Fig. 6), suggesting that CLIC5A and PI(4,5)P_2-generating kinases can associate in cells. Some cells in cultures transfected with CLIC5A developed large intracellular vacuoles (Fig. 6D) similar those described previously in cells overexpressing PI4P5Kα (Yonemura et al., 2002). These vacuoles were observed whether CLIC5A was expressed with or without exogenous HA–PI4P5Kα, but never in vector-transfected cells lacking CLIC5A. We observed that CLIC5A and HA–PI4P5Kα colocalized at the membranes of these large vacuoles, and that PI(4,5)P_2 accumulated at that location (Fig. 6E). Therefore, there appears to be a close association of CLIC5A with PI4P5Kα at locations of enhanced PI(4,5)P_2 generation in CLIC5A-transfected cells. These findings are consistent with a yeast two-hybrid screen that has suggested a possible direct interaction between the C-terminal region of PI4P5Kβ and both CLIC1 and CLIC4 (http://www.signaling-gateway.org). Furthermore, Ikenouchi et al. (Ikenouchi et al., 2013) have shown that PI4P5Kβ associates with NHERF2 in a podocalyxin–NHERF2 complex. Our studies suggest that CLIC5A can interact with all isoforms of PI4P5K and PI5P5K, but because we did not identify the specific endogenous kinase that interacts with CLIC5A in podocytes, it is possible that the effect of CLIC5A on ERM phosphorylation *in vivo* is restricted to PI4P5Kβ. Although proof of a direct interaction between CLIC5A and PI(4,5)P_2-generating kinases is still lacking, the finding that silencing of endogenous PI4P5Kα abrogates CLIC5A-induced ERM phosphorylation (Fig. 7A) strongly suggests that, in COS-7 cells, CLIC5A directs PI4P5Kα-dependent PI(4,5)P_2 accumulation to sites where ERM proteins can then dock.

When exogenous HA–PIP5Kα was expressed in COS-7 cells, it localized to the dorsal plasma membrane of COS-7 cells even in the absence of CLIC5A. Furthermore, HA–PIP5Kα was also found at the dorsal plasma membrane in the presence of CLIC5A truncation mutants (22–251, 55–251 and 1–232) that remained cytosolic. Therefore, it seems unlikely that CLIC5A is required for the recruitment of PIP5Kα to a plasma membrane location. Nonetheless, even though overexpressed PIP5Kα was observed at the plasma membrane in the absence of CLIC5A, and in the presence of the CLIC5A mutants, we only observed enhanced clustered PI(4,5)P_2 accumulation (Fig. 7D) and ERM phosphorylation (Fig. 7B) in the presence of full-length CLIC5A. Hence, PIP5Kα membrane association did not depend on CLIC5A, but the generation of PI(4,5)P_2 and its downstream effect on ERM phosphorylation did. This finding is most consistent with a model in which CLIC5A increases the localized activity of PI(4,5)P_2-generating enzymes, rather than simply recruiting them to the plasma membrane. Because the abundance of endogenous PI(4,5)P_2-generating enzymes was too low for detection by co-immunoprecipitation or colocalization in this study, it remains unclear whether CLIC5A associates with and activates a specific isoform. Taken together with our evidence of increased clustered accumulation of PI(4,5)P_2 at the dorsal plasma membrane, increased PI(4,5)P_2-dependent ERM phosphorylation in the presence of CLIC5A and the formation of surface ruffles and projections in CLIC5A-expressing cells, it is attractive to postulate that the mechanism of CLIC5A action involves activation of PI4P5K and/or PI5P4K with consequent PI(4,5)P_2 generation that, in turn, facilitates ERM phosphorylation. It is also possible that CLIC5A forms a scaffold that helps assemble proteins involved in activating PI4P5 and/or PI5P4 kinases in specific compartments of the phospholipid bilayer involved in the formation of ERM-dependent projections.

Finally, we evaluated the functional effect of CLIC5A on phosphorylation of ERM protein in renal glomeruli *in vivo*. In glomerular podocytes, ezrin serves to couple the single transmembrane sialoglycoprotein podocalyxin to cortical actin, through the intermediate NHERF2 (Takeda, 2003; Takeda et al., 2001). There was a striking reduction of phospho-ERM and ezrin in the detergent-insoluble fraction prepared from glomeruli of CLIC5-deficient compared with wild-type mice, in keeping with our findings in the COS-7 cells, and our previous finding of reduced phospho-ERM by immunofluorescence microscopy (Wegner et al., 2010). Furthermore, the association of NHERF-2 with the detergent-insoluble fraction was markedly reduced in the CLIC5-deficient mice. The work in glomeruli of CLIC5-deficient mice is consistent with the findings in COS-7 cells and suggests that CLIC5A is a functionally important component of the podocalyxin–NHERF2–ezrin complex that is required for ezrin activation and coupling of the podocalyxin–NHERF2 complex to the actin cytoskeleton, in turn, supporting the normal foot process architecture.

Taken together, the findings in cultured cells and *in vivo* are consistent with a model (Fig. 8D) whereby CLIC5A associates with the apical plasma membrane of podocyte foot processes where it supports clustered PI(4,5)P_2 generation in a highly localized fashion. PI(4,5)P_2 in turn engages the ezrin N-terminus, resulting in a conformational change in ezrin that then allows the ezrin N-terminus to bind to NHERF2, and its C-terminus to bind to actin. The conformational change of ezrin induced by CLIC5A-dependent PI(4,5)P_2 generation would also promote PKC-mediated phosphorylation of the ezrin at Thr567 (Fig. 8D). Further work is required to determine whether CLIC5A directly binds to and activates PI(4,5)P_2-generating kinase(s), or whether it serves as a scaffolding platform that assembles the appropriate components of the PI(4,5)P_2 signaling complex. It is also still unclear which of the PI4P5 or PI5P4 kinases interacts with CLIC5A in podocytes *in vivo*.

MATERIALS AND METHODS

Reagents and antibodies

All chemicals were of reagent grade and purchased from Sigma (Oakville, ON, Canada) unless otherwise noted. Rabbit anti-phospho-Thr567 ezrin antibodies were from Signalway Antibody LLC (SAB; College Park, MD), and mouse anti-phospho-Thr567 ezrin antibodies were from BD Biosciences (Franklin Lakes, NJ). The anti-phospho-Thr567 ezrin antibodies crossreact with phosphorylated radixin and moesin. Signals obtained with these antibodies are therefore referred to as phosphorylated ERM (phospho-ERM). Rabbit anti-ezrin and anti-PI4P5Kα antibodies were from Cell Signaling (Danvers, MA), rabbit anti-CLIC5 antibodies were from Aviva System Biology (San Diego, CA), mouse anti-β-tubulin and anti-β-actin antibodies were from Millipore (Billerica, MA) and Sigma (Oakville, ON, Canada) respectively. Calyculin A (Cal-A) and m-3M3FBS and were from

Journal of Cell Science (2014) 127, 5164–5178 doi:10.1242/jcs.147744

Millipore (Billerica, MA). Goat anti-podocalyxin antibodies were from R&D Systems (Minneapolis, MN), rat anti-HA antibodies were from Roche (Indianapolis, IN) and goat anti-NHERF2 antibodies were from Santa Cruz Biotechnology Inc. (Dallas, TX).

Cell culture and transfection

COS-7 and HeLa cells were maintained in Dulbecco's Modified Eagles Medium (DMEM) containing 10% fetal bovine serum (FBS) (Life Technologies, Burlington, ON) in a 37℃ and 5% CO_2 humidified incubator. COS-7 cells were derived from CV-1 cells (Gluzman, 1981) that, in turn, were originally derived from green monkey kidney epithelial cells (Jensen et al., 1964). However, because COS-7 cells are not well polarized, we refer to the cell surface facing the medium as 'dorsal' throughout. Cells in six-well or P35 dishes were transfected with 4 µg of plasmid construct using Lipofectamine 2000 (Life Technologies) for COS-7 or Lipofectamine LTX (Life Technologies) for HeLa cells according to the manufacturer's instruction. To maximize the probability of CLIC5A expression with reporter constructs (YFP–actin, GFP–PH-PLC and GFP–Kras), cells were transfected with a mixture of 4 µg CLIC5A and 0.4 µg reporter construct cDNA (ratio of CLIC5A:reporter of 10:1). To prepare cell lysates, cells in P35 plates were washed twice with ice-cold PBS 2 days after transfection and then scraped into 500 µl Triton X-100 lysis buffer [0.5% Triton X-100, 10 mM HEPES pH 7.0, 100 mM NaCl, 2.5 mM EGTA, 5 mM $MgCl_2$, 100 nM Cal-A and 1× PhosStop (Pierce)]. To prepare total SDS-soluble cell lysates, the material in the Triton X-100 buffer was evenly suspended and 100 µl was placed into 2× Laemmli buffer containing 14 mM 2-mercaptoethanol and boiled for 5 min. To harvest the Triton-X-100-insoluble proteins, the remaining 400 µl of the material in Triton X-100 lysis buffer was centrifuged at 18,000 ***g*** for 30 min at 4℃. The supernatant was removed and the Triton-X-100-insoluble fraction was resuspended in 100 µl of Laemmli buffer and boiled for 5 min. For some experiments, COS-7 cells were plated in six-well plates on the day prior to transfection, transfected with either CLIC5A or vector and treated 48 h later with 100 nM staurosporine (SSP), 15 µM Y-27632 or 100 nM Cal-A. After the appropriate period of incubation, cells were washed twice with ice-cold PBS and harvested as described.

Plasmid constructs and CLIC5A cloning

Constructs encoding the PI(4,5)P_2 reporters (GFP–PH-PLC and RFP–PH-PLC) and negative charge biosensor (GFP–Kras) were obtained from Sergio Grinstein (University of Toronto, Canada). Constructs encoding the HA–PI4,5P kinases were provided by Greg Longmore (Washington University School of Medicine, St Louis, MO) and the YFP–actin construct was provided by Allan Murray (University of Alberta, Canada). A cDNA for CLIC5A encoding the complete open reading frame (ORF) (GenBank™ number DQ679794) was PCR amplified from human kidney cDNA with the primers 5′-CGCACTCGAG**ACCATGG**GGG*CATCATCATCATCATCAT*ACAGACTCGGCGACAGCTAAC-3′ (forward) and 5′-CCGGGATCCTCAGGATCGGCTGAGGCGTTTGGC-3′ (reverse). In the forward primer, one Kozak consensus sequence (bold) was added to enhance expression and a 6×His tag sequence (italic) was integrated for detection. The PCR product was directly cloned into pCDNA3.1/V5-his-TOPO vector (Life Technologies). This construct is designated pcDNA3.1-CLIC5A (or CLIC5A in the figure legends). The GFP–CLIC5A construct was generated by PCR amplification of human CLIC5A full coding region from pcDNA3.1-CLIC5A using the primers 5′-CGCACTCGAGCCATGACAGACTCGGCGACAGCTAAC-3′ (forward) and 5′-CCGGGATCCTCAGGATCGGCTGAGGCGTTTGGC-3′ (reverse), and cloning into the *Xho*I-*Bam*HI site of the pEGFP-C1 vector (Clontech, Mountain View, CA). Xpress-tagged wild-type CLIC5A (1–251) and truncation deletion cDNAs (22–251, first β-pleated sheet deletion; 55–251, first β-pleated sheet and putative transmembrane domain deletion; and 1–232, number 9 helix domain deletion) were PCR amplified from pCDNA3.1-CLIC5A using the primers 5′-AGCTTCATGGGGGATCTGTACGACGATGACGATAAGACAGACTCGGCGACAGCTAACGGG-3′ (forward for 1–251 and 1–232), 5′-GCTTCATGGGGGATCTGTACGACGATGACGATAAGGCTGGAATCGATGGAGAAAGCATC-3′ (forward for 22–251), 5′-AGCTTCATGGGGGATCTGTACGACGATGACGATAAGGATCTGAAAAGAAAGCCAGCTGAC-3′ (forward for 55–251), 5′-CCGGGATCCTCAGGATCGGCTGAGGCGTTTGGC-3′ (reverse for 1–251, 22–251 and 55–251) and 5′-CCGGGATCCTCATGCACAGGTGTTGGTGAACTCATC-3′ (reverse for 1–232), followed by cloning into pTARGET vector (Promega, Madison, WI). Restriction enzyme digestion and full-insert sequencing verified the DNA sequence orientation and fidelity.

GST–CLIC5A construct, bacterial expression and the recombinant protein purification

The full coding region of human CLIC5A was amplified from the pCDNA3.1-CLIC5A construct using PCR with the primers 5′-CGTGGGATCCCCATGACAGACTCGGCGACAGCTAAC-3′ (forward) and 5′-CCGGAATTCTCAGGATCGGCTGAGGCGTTTGGC-3′ (reverse). The PCR-derived CLIC5A was cloned into pGEX-3 (GE Healthcare, Piscataway, NJ). The DNA sequences were verified by sequencing. *Escherichia coli* BL21 Gold (DE3) (Agilent Technologies, Santa Clara, CA) were transformed with pGEX-3 or pGEX-CLIC5A constructs, induced with 0.2 mM IPTG and grown at 37℃ for 4 h. Cells were harvested in PBS containing 1× proteinase inhibitor cocktail (Roche Diagnostics, Indianapolis, IN), followed by sonication and addition of Triton X-100 to a final concentration of 1%. GST and GST–CLIC5A proteins were purified by affinity chromatography on glutathione−Sepharose 4B (GE Healthcare) according the manufacturer's protocol.

siRNA-mediated silencing

To silence PI4P5Kα expression, control siRNA (sc-37007) or PI4P5Kα-specific siRNA (-sc-36232) were purchased from Santa Cruz Biotechnology. The PI4P5Kα siRNA mix consisted of equal concentrations of three distinct siRNAs targeting 5′-GAAGAACCGGAUUGAAAGA-3′, 5′-CAACCUCAUCAGCCUUGAA-3′ and 5′-CCUUCCUCUUCCUCAUGAA-3′ of the human PI4P5Kα mRNA sequence. COS-7 or HeLa cells were plated in 35-mm plates at approximately 60% confluence the day prior to transfection. The medium was replaced with 1 ml of medium without antibiotics immediately before transfection. A total of 2–3 µg of CLIC5A or vector plasmid with 6 pmol control or PI4P5Kα siRNA were combined with 4 µl of Lipofectamine 2000 in 100 µl of Opti-MEM I medium (Life Technologies), co-incubated at room temperature for 45 min and then added to the cells. At 6 h later, 1 ml of growth medium containing 20% FBS was added to the cells. The medium was replaced with serum-free medium (6–10 h) prior to lysis at 48 h after initiation of the transfection.

Cytoskeleton preparation

Cell cytoskeletal fractions were prepared as described previously (Berryman et al., 2004). Briefly, cells in P35 plates were washed twice on ice with cold PBS containing 5 nM Cal-A, and were then incubated at room temperature in 500 µl of PBS containing 0.5% Triton X-100, 1× complete proteinase inhibitor, 1× PhosStop (Roche) and 100 nM Cal-A. The supernatant was removed and the cells were washed gently twice with cold PBS to remove solubilized material. The resulting cytoskeletons were collected in 200 µl of Laemmli buffer and boiled for 5 min prior to western blotting.

Western blot analysis and quantification

Protein samples were boiled for 5 min in Laemmli buffer containing β-mercaptoethanol. They were then separated by electrophoresis on a 12% SDS-PAGE and transferred to polyvinylidene fluoride (PVDF) membranes. Membranes were blocked, incubated with the appropriate primary and HRP-conjugated secondary antibodies and developed with enhanced chemiluminescence (ECL; GE Amersham, Baie d'Urfe, QC, Canada). The membranes were then exposed to X-ray film (Fuji Medical X-Ray Film Super Rx, Fujifilm) for several different time periods. Band density was evaluated using Quantity One software (Biorad Mississauga, ON, Canada). Protein loading was controlled by probing with anti-tubulin or anti-β-actin antibodies.

Immunofluorescence microscopy

Cells grown on glass coverslips were washed with cold PBS on ice and fixed with 10% trichloroacetic acid (TCA) to preserve ERM

phosphorylation (Hayashi et al., 1999) for 15 min at room temperature. Cells were permeabilized with 0.05% Triton X-100 in PBS for 15 min, blocked with PBS containing 5% goat serum and incubated with primary antibodies overnight at 4℃. The cells were washed four to six times with PBS containing 30 mM glycine (G-PBS) and incubated with secondary antibodies for 1 h at room temperature, followed by three G-PBS washes and mounting in Prolong Antifade (Life Technologies). For actin staining, cells were fixed with 4% paraformaldehyde in PBS for 15 min at room temperature, washed three times with PBS and blocked with PBS containing 5% goat serum for 1 h at room temperature. Cells were then incubated with Rhodamine–phalloidin for 30 min at room temperature, washed with PBS and mounted in Prolong Antifade. For live-cell imaging, COS-7 cells grown on 25-mm glass coverslips were placed into the imaging chamber (37℃, 5% CO_2) of an Olympus spinning-disk fluorescence microscope (Olympus IX-81), and image acquisition was performed with Volocity (Improvision) software. Quantification of the plasma membrane:cytosol ratio of GFP–PH-PLC (Fig. 4B) was performed using ImageJ (National Institutes of Health). For each cell, the green pixel density was determined in the *X*-*Z* optical sections using three uniform squares overlaid on cytosol, dorsal plasma membrane (cell apex and immediately left and right) and outside the cell (background). After subtraction of background, the mean density was determined for cytosol and plasma membrane and the ratio was determined. Quantification was performed for ten cells in each of three independent experiments.

Scanning electron microscopy

Cells were fixed with 2% glutaraldehyde for 15 min, washed twice with PBS and dehydrated in a graded series of ethanol (30%, 50%, 70%, 95% and 100%). After dehydration, cells were passed through a serial dilution of hexamethyldisilazane (HMDS) in ethanol (75% ethanol, 25% HMDS; 50% ethanol, 50% HMDS; 25% ethanol, 75% HMDS) and 100% HMDS, dried, mounted on SEM stubs and sputter-coated with Au/Pd. Samples were imaged with a Philips/FEI (XL30) scanning electron microscope.

GST-pulldown assay

The GST-pull down assay was performed as described previously (Berryman and Bretscher, 2000) with some modifications. Briefly, COS-7 cells expressing HA–PI4P5 or HA–PI5P4 kinases were lysed for 20 min in buffer containing 1% Triton X-100, 20 mM HEPES pH 7.4, 0.6 M KCl and 1 mM EDTA, followed by centrifugation for 30 min at 20,800 ***g***. The clarified supernatant was diluted six times in buffer containing 20 mM HEPES pH 7.4, 10 mM $MgCl_2$, 1.0 mM ATP, 1× proteinase inhibitor complex and PhosStop. A total of 100 µl was taken as input and the rest was diluted and incubated with GST or GST–CLIC5A immobilized on glutathione beads on a rotator for 3 h at room temperature. The beads were washed five times (for 3 min each) with buffer containing 20 mM HEPES pH 7.4, 100 mM NaCl and 0.1% Triton X-100. Bound proteins were eluted in 2× Laemmli buffer followed by western blotting using anti-HA antibodies.

Studies in CLIC5-deficient mice

The CLIC5-deficient C57/BL6 mice were derived from the original $CLIC5^{jbg/jbg}$ strain on the C3H/HeJ background (Gagnon et al., 2006; Wegner et al., 2010), by crossing them for more than ten generations into the C57/BL6 background. All procedures in mice were approved by the University of Alberta Animal Care and Use Committee (protocol number 545). Genotyping and immunofluorescence studies were performed as described previously (Wegner et al., 2010). Renal cortex was isolated, minced with a razor blade and incubated for in RPMI 1640 medium containing 10 nM calyculin A and 1 mg/ml collagenase IV (Worthington, Lakewood, NJ) for 1 h at 37℃. Glomeruli were then isolated with the sieving technique as described previously (Skorecki et al., 1983). Contaminating tubules were removed by differential adhesion to cell culture plastic during two successive 10-min periods of incubation in RPMI 1640 medium containing 0.5% FBS and 10 nM calyculin A. The final glomerular preparations were >99% pure. Glomeruli were then sedimented by centrifugation at 1000 ***g*** for 5 min and resuspended in lysis buffer (50 mM Tris-HCl pH 7.5, 150 mM NaCl, 1% Nonidet P40, 0.5% sodium deoxycholate, 1× proteinase inhibitor mix, 1× PhosStop and 100 nM Calyculin A). After incubation on ice for 15 min, glomeruli were gently homogenized by passing them through a 28-gauge needle three times. The detergent-insoluble fraction was pelleted by centrifugation at 18,000 ***g*** for 10 min. Detergent soluble and insoluble fractions were resuspended in Laemmli buffer, boiled for 5 min and processed for western blot analysis. For NHERF2 studies, renal cortex was isolated from the renal medulla, finely minced with a razor blade and suspended in calyculin-A-containing lysis buffer as for glomeruli. The cortex was homogenized (PowerGen, Fisher Scientific). The material was then subjected to centrifugation at 14,000 ***g*** for 30 min at 4℃. The detergent-soluble and -insoluble fractions were then suspended in Laemmli buffer, boiled for 5 min and processed for western blot analysis.

Acknowledgements

The HA–PI4P5 and HA–PI5P4 kinase constructs were kindly provided by Greg Longmore (Washington University School of Medicine, St Louis, MO).

Competing interests

The authors declare no competing interests.

Author contributions

A.A.-M. and L.L. performed essentially all of the experiments and prepared a near-final draft of the manuscript. R.T.A. helped to design and interpret $PI(4,5)P_2$ and negative-charge reporter assays. As principal investigator, B.J.B. designed the overall experimental approach, supervised the studies and prepared the final draft of the paper. All authors approved the final version of the manuscript.

Funding

B.J.B. was supported by operating funds from Canadian Institutes of Health Research (CIHR) [grant number MOP 641814]; and the Kidney Foundation of Canada (KFOC). R.T.A. is supported by operating funds from KFOC and by a Clinician Scientist Award from CIHR and a Clinical Investigator Award from Alberta Innovates-Health Solutions. The Division of Nephrology provided support for tuition and core infrastructure.

References

Ashley, R. H. (2003). Challenging accepted ion channel biology: p64 and the CLIC family of putative intracellular anion channel proteins. (Review). *Mol. Membr. Biol.* **20**, 1-11.

Barret, C., Roy, C., Montcourrier, P., Mangeat, P. and Niggli, V. (2000). Mutagenesis of the phosphatidylinositol 4,5-bisphosphate (PIP(2)) binding site in the NH(2)-terminal domain of ezrin correlates with its altered cellular distribution. *J. Cell Biol.* **151**, 1067-1080.

Baumgartner, M., Sillman, A. L., Blackwood, E. M., Srivastava, J., Madson, N., Schilling, J. W., Wright, J. H. and Barber, D. L. (2006). The Nck-interacting kinase phosphorylates ERM proteins for formation of lamellipodium by growth factors. *Proc. Natl. Acad. Sci. USA* **103**, 13391-13396.

Berry, K. L., Bülow, H. E., Hall, D. H. and Hobert, O. (2003). A C. elegans CLIC-like protein required for intracellular tube formation and maintenance. *Science* **302**, 2134-2137.

Berryman, M. and Bretscher, A. (2000). Identification of a novel member of the chloride intracellular channel gene family (CLIC5) that associates with the actin cytoskeleton of placental microvilli. *Mol. Biol. Cell* **11**, 1509-1521.

Berryman, M., Bruno, J., Price, J. and Edwards, J. C. (2004). CLIC-5A functions as a chloride channel in vitro and associates with the cortical actin cytoskeleton in vitro and in vivo. *J. Biol. Chem.* **279**, 34794-34801.

Bretscher, A. (1999). Regulation of cortical structure by the ezrin-radixin-moesin protein family. *Curr. Opin. Cell Biol.* **11**, 109-116.

Bretscher, A., Edwards, K. and Fehon, R. G. (2002). ERM proteins and merlin: integrators at the cell cortex. *Nat. Rev. Mol. Cell Biol.* **3**, 586-599.

Canals, D., Roddy, P. and Hannun, Y. A. (2012). Protein phosphatase 1α mediates ceramide-induced ERM protein dephosphorylation: a novel mechanism independent of phosphatidylinositol 4, 5-biphosphate (PIP2) and myosin/ERM phosphatase. *J. Biol. Chem.* **287**, 10145-10155.

Chuang, J. Z., Milner, T. A., Zhu, M. and Sung, C. H. (1999). A 29 kDa intracellular chloride channel p64H1 is associated with large dense-core vesicles in rat hippocampal neurons. *J. Neurosci.* **19**, 2919-2928.

Cromer, B. A., Morton, C. J., Board, P. G. and Parker, M. W. (2002). From glutathione transferase to pore in a CLIC. *Eur. Biophys. J.* **31**, 356-364.

Cromer, B. A., Gorman, M. A., Hansen, G., Adams, J. J., Coggan, M., Littler, D. R., Brown, L. J., Mazzanti, M., Breit, S. N., Curmi, P. M. et al. (2007). Structure of the Janus protein human CLIC2. *J. Mol. Biol.* **374**, 719-731.

Denker, S. P. and Barber, D. L. (2002). Cell migration requires both ion translocation and cytoskeletal anchoring by the Na-H exchanger NHE1. *J. Cell Biol.* **159**, 1087-1096.

Denker, S. P., Huang, D. C., Orlowski, J., Furthmayr, H. and Barber, D. L. (2000). Direct binding of the Na-H exchanger NHE1 to ERM proteins regulates the cortical cytoskeleton and cell shape independently of H(+) translocation. *Mol. Cell* **6**, 1425-1436.
Divecha, N. (2010). Lipid kinases: charging PtdIns(4,5)P2 synthesis. *Curr. Biol.* **20**, R154-R157.
Edwards, J. C., Cohen, C., Xu, W. and Schlesinger, P. H. (2006). c-Src control of chloride channel support for osteoclast HCl transport and bone resorption. *J. Biol. Chem.* **281**, 28011-28022.
Fairn, G. D., Ogata, K., Botelho, R. J., Stahl, P. D., Anderson, R. A., De Camilli, P., Meyer, T., Wodak, S. and Grinstein, S. (2009). An electrostatic switch displaces phosphatidylinositol phosphate kinases from the membrane during phagocytosis. *J. Cell Biol.* **187**, 701-714.
Fernández-Salas, E., Sagar, M., Cheng, C., Yuspa, S. H. and Weinberg, W. C. (1999). p53 and tumor necrosis factor alpha regulate the expression of a mitochondrial chloride channel protein. *J. Biol. Chem.* **274**, 36488-36497.
Fievet, B. T., Gautreau, A., Roy, C., Del Maestro, L., Mangeat, P., Louvard, D. and Arpin, M. (2004). Phosphoinositide binding and phosphorylation act sequentially in the activation mechanism of ezrin. *J. Cell Biol.* **164**, 653-659.
Gagnon, L. H., Longo-Guess, C. M., Berryman, M., Shin, J. B., Saylor, K. W., Yu, H., Gillespie, P. G. and Johnson, K. R. (2006). The chloride intracellular channel protein CLIC5 is expressed at high levels in hair cell stereocilia and is essential for normal inner ear function. *J. Neurosci.* **26**, 10188-10198.
Gluzman, Y. (1981). SV40-transformed simian cells support the replication of early SV40 mutants. *Cell* **23**, 175-182.
Goodchild, S. C., Howell, M. W., Cordina, N. M., Littler, D. R., Breit, S. N., Curmi, P. M. and Brown, L. J. (2009). Oxidation promotes insertion of the CLIC1 chloride intracellular channel into the membrane. *Eur. Biophys. J.* **39**, 129-138.
Grune, T., Reinheckel, T., North, J. A., Li, R., Bescos, P. B., Shringarpure, R. and Davies, K. J. (2002). Ezrin turnover and cell shape changes catalyzed by proteasome in oxidatively stressed cells. *FASEB J.* **16**, 1602-1610.
Hao, J. J., Liu, Y., Kruhlak, M., Debell, K. E., Rellahan, B. L. and Shaw, S. (2009). Phospholipase C-mediated hydrolysis of PIP2 releases ERM proteins from lymphocyte membrane. *J. Cell Biol.* **184**, 451-462.
Hayashi, K., Yonemura, S., Matsui, T. and Tsukita, S. (1999). Immunofluorescence detection of ezrin/radixin/moesin (ERM) proteins with their carboxyl-terminal threonine phosphorylated in cultured cells and tissues. *J. Cell Sci.* **112**, 1149-1158.
Hirao, M., Sato, N., Kondo, T., Yonemura, S., Monden, M., Sasaki, T., Takai, Y., Tsukita, S. and Tsukita, S. (1996). Regulation mechanism of ERM (ezrin/radixin/moesin) protein/plasma membrane association: possible involvement of phosphatidylinositol turnover and Rho-dependent signaling pathway. *J. Cell Biol.* **135**, 37-51.
Ikenouchi, J., Hirata, M., Yonemura, S. and Umeda, M. (2013). Sphingomyelin clustering is essential for the formation of microvilli. *J. Cell Sci.* **126**, 3585-3592.
Ivetic, A. and Ridley, A. J. (2004). Ezrin/radixin/moesin proteins and Rho GTPase signalling in leucocytes. *Immunology* **112**, 165-176.
Jensen, F. C., Girardi, A. J., Gilden, R. V. and Koprowski, H. (1964). Infection of human and simian tissue cultures with Rous Sarcoma virus. *Proc. Natl. Acad. Sci. USA* **52**, 53-59.
Jentsch, T. J., Stein, V., Weinreich, F. and Zdebik, A. A. (2002). Molecular structure and physiological function of chloride channels. *Physiol. Rev.* **82**, 503-568.
Jiang, L., Salao, K., Li, H., Rybicka, J. M., Yates, R. M., Luo, X. W., Shi, X. X., Kuffner, T., Tsai, V. W., Husaini, Y. et al. (2012). Intracellular chloride channel protein CLIC1 regulates macrophage function through modulation of phagosomal acidification. *J. Cell Sci.* **125**, 5479-5488.
Jiang, L., Phang, J. M., Yu, J., Harrop, S. J., Sokolova, A. V., Duff, A. P., Wilk, K. E., Alkhamici, H., Breit, S. N., Valenzuela, S. M. et al. (2014). CLIC proteins, ezrin, radixin, moesin and the coupling of membranes to the actin cytoskeleton: a smoking gun? *Biochim. Biophys. Acta* **1838**, 643-657.
Khanna, C., Wan, X., Bose, S., Cassaday, R., Olomu, O., Mendoza, A., Yeung, C., Gorlick, R., Hewitt, S. M. and Helman, L. J. (2004). The membrane-cytoskeleton linker ezrin is necessary for osteosarcoma metastasis. *Nat. Med.* **10**, 182-186.
Kitajiri, S., Fukumoto, K., Hata, M., Sasaki, H., Katsuno, T., Nakagawa, T., Ito, J., Tsukita, S. and Tsukita, S. (2004). Radixin deficiency causes deafness associated with progressive degeneration of cochlear stereocilia. *J. Cell Biol.* **166**, 559-570.
Lamb, R. F., Ozanne, B. W., Roy, C., McGarry, L., Stipp, C., Mangeat, P. and Jay, D. G. (1997). Essential functions of ezrin in maintenance of cell shape and lamellipodial extension in normal and transformed fibroblasts. *Curr. Biol.* **7**, 682-688.
Landry, D., Sullivan, S., Nicolaides, M., Redhead, C., Edelman, A., Field, M., al-Awqati, Q. and Edwards, J. (1993). Molecular cloning and characterization of p64, a chloride channel protein from kidney microsomes. *J. Biol. Chem.* **268**, 14948-14955.
Littler, D. R., Harrop, S. J., Fairlie, W. D., Brown, L. J., Pankhurst, G. J., Pankhurst, S., DeMaere, M. Z., Campbell, T. J., Bauskin, A. R., Tonini, R. et al. (2004). The intracellular chloride ion channel protein CLIC1 undergoes a redox-controlled structural transition. *J. Biol. Chem.* **279**, 9298-9305.
Littler, D. R., Assaad, N. N., Harrop, S. J., Brown, L. J., Pankhurst, G. J., Luciani, P., Aguilar, M. I., Mazzanti, M., Berryman, M. A., Breit, S. N. et al. (2005). Crystal structure of the soluble form of the redox-regulated chloride ion channel protein CLIC4. *FEBS J.* **272**, 4996-5007.
Littler, D. R., Harrop, S. J., Goodchild, S. C., Phang, J. M., Mynott, A. V., Jiang, L., Valenzuela, S. M., Mazzanti, M., Brown, L. J., Breit, S. N. et al. (2010). The enigma of the CLIC proteins: Ion channels, redox proteins, enzymes, scaffolding proteins? *FEBS Lett.* **584**, 2093-2101.
Machesky, L. M. (2008). Lamellipodia and filopodia in metastasis and invasion. *FEBS Lett.* **582**, 2102-2111.
Matsui, T., Yonemura, S., Tsukita, S. and Tsukita, S. (1999). Activation of ERM proteins in vivo by Rho involves phosphatidyl-inositol 4-phosphate 5-kinase and not ROCK kinases. *Curr. Biol.* **9**, 1259-1262, S1-S3.
Niggli, V., Andréoli, C., Roy, C. and Mangeat, P. (1995). Identification of a phosphatidylinositol-4,5-bisphosphate-binding domain in the N-terminal region of ezrin. *FEBS Lett.* **376**, 172-176.
Niggli, H. J., Scaletta, C., Yu, Y., Popp, F. A. and Applegate, L. A. (2001). Ultraweak photon emission in assessing bone growth factor efficiency using fibroblastic differentiation. *J. Photochem. Photobiol. B* **64**, 62-68.
Nyström, J., Fierlbeck, W., Granqvist, A., Kulak, S. C. and Ballermann, B. J. (2009). A human glomerular SAGE transcriptome database. *BMC Nephrol.* **10**, 13.
Orlando, R. A., Takeda, T., Zak, B., Schmieder, S., Benoit, V. M., McQuistan, T., Furthmayr, H. and Farquhar, M. G. (2001). The glomerular epithelial cell anti-adhesin podocalyxin associates with the actin cytoskeleton through interactions with ezrin. *J. Am. Soc. Nephrol.* **12**, 1589-1598.
Orlando, G. S., Tobey, N. A., Wang, P., Abdulnour-Nakhoul, S., Orlando, R. C. (2002). Regulatory volume decrease in human esophageal epithelial cells. *Am. J. Physiol.* **283**, G932-G937
Pierchala, B. A., Muñoz, M. R. and Tsui, C. C. (2010). Proteomic analysis of the slit diaphragm complex: CLIC5 is a protein critical for podocyte morphology and function. *Kidney Int.* **78**, 868-882.
Rameh, L. E., Tolias, K. F., Duckworth, B. C. and Cantley, L. C. (1997). A new pathway for synthesis of phosphatidylinositol-4,5-bisphosphate. *Nature* **390**, 192-196.
Redhead, C. R., Edelman, A. E., Brown, D., Landry, D. W. and al-Awqati, Q. (1992). A ubiquitous 64-kDa protein is a component of a chloride channel of plasma and intracellular membranes. *Proc. Natl. Acad. Sci. USA* **89**, 3716-3720.
Salles, F. T., Andrade, L., Tanda, S., Grati, M., Plona, K. L., Gagnon, L. H., Johnson, K. R., Kachar, B. and Berryman, M. A. (2013). CLIC5 stabilizes membrane-actin filament linkages at the base of hair cell stereocilia in a molecular complex with Radixin, Taperin, and Myosin VI. *Cytoskeleton (Hoboken)* **71**, 61-78.
Schwartz-Albiez, R., Merling, A., Spring, H., Möller, P. and Koretz, K. (1995). Differential expression of the microspike-associated protein moesin in human tissues. *Eur. J. Cell Biol.* **67**, 189-198.
Shanks, R. A., Larocca, M. C., Berryman, M., Edwards, J. C., Urushidani, T., Navarre, J. and Goldenring, J. R. (2002). AKAP350 at the Golgi apparatus. II. Association of AKAP350 with a novel chloride intracellular channel (CLIC) family member. *J. Biol. Chem.* **277**, 40973-40980.
Shibasaki, Y., Ishihara, H., Kizuki, N., Asano, T., Oka, Y. and Yazaki, Y. (1997). Massive actin polymerization induced by phosphatidylinositol-4-phosphate 5-kinase in vivo. *J. Biol. Chem.* **272**, 7578-7581.
Shiue, H., Musch, M. W., Wang, Y., Chang, E. B. and Turner, J. R. (2005). Akt2 phosphorylates ezrin to trigger NHE3 translocation and activation. *J. Biol. Chem.* **280**, 1688-1695.
Singh, H., Cousin, M. A. and Ashley, R. H. (2007). Functional reconstitution of mammalian 'chloride intracellular channels' CLIC1, CLIC4 and CLIC5 reveals differential regulation by cytoskeletal actin. *FEBS J.* **274**, 6306-6316.
Skorecki, K. L., Ballermann, B. J., Rennke, H. G. and Brenner, B. M. (1983). Angiotensin II receptor regulation in isolated renal glomeruli. *Fed. Proc.* **42**, 3064-3070.
Takeda, T. (2003). Podocyte cytoskeleton is connected to the integral membrane protein podocalyxin through Na+/H+-exchanger regulatory factor 2 and ezrin. *Clin. Exp. Nephrol.* **7**, 260-269.
Takeda, T., McQuistan, T., Orlando, R. A. and Farquhar, M. G. (2001). Loss of glomerular foot processes is associated with uncoupling of podocalyxin from the actin cytoskeleton. *J. Clin. Invest.* **108**, 289-301.
Takeuchi, K., Sato, N., Kasahara, H., Funayama, N., Nagafuchi, A., Yonemura, S., Tsukita, S. and Tsukita, S. (1994). Perturbation of cell adhesion and microvilli formation by antisense oligonucleotides to ERM family members. *J. Cell Biol.* **125**, 1371-1384.
Tsukita, S. and Yonemura, S. (1997). ERM (ezrin/radixin/moesin) family: from cytoskeleton to signal transduction. *Curr. Opin. Cell Biol.* **9**, 70-75.
Tsukita, S. and Yonemura, S. (1999). Cortical actin organization: lessons from ERM (ezrin/radixin/moesin) proteins. *J. Biol. Chem.* **274**, 34507-34510.
Tulk, B. M., Schlesinger, P. H., Kapadia, S. A. and Edwards, J. C. (2000). CLIC-1 functions as a chloride channel when expressed and purified from bacteria. *J. Biol. Chem.* **275**, 26986-26993.
Ulmasov, B., Bruno, J., Gordon, N., Hartnett, M. E. and Edwards, J. C. (2009). Chloride intracellular channel protein-4 functions in angiogenesis by supporting acidification of vacuoles along the intracellular tubulogenic pathway. *Am. J. Pathol.* **174**, 1084-1096.
Valenzuela, S. M., Alkhamici, H., Brown, L. J., Almond, O. C., Goodchild, S. C., Carne, S., Curmi, P. M., Holt, S. A. and Cornell, B. A. (2013). Regulation of the membrane insertion and conductance activity of the metamorphic chloride intracellular channel protein CLIC1 by cholesterol. *PLoS ONE* **8**, e56948.
Viswanatha, R., Wayt, J., Ohouo, P. Y., Smolka, M. B. and Bretscher, A. (2013). Interactome analysis reveals ezrin can adopt multiple conformational states. *J. Biol. Chem.* **288**, 35437-35451.

Journal of Cell Science (2014) 127, 5164–5178 doi:10.1242/jcs.147744

Wade, J. B., Welling, P. A., Donowitz, M., Shenolikar, S. and Weinman, E. J. (2001). Differential renal distribution of NHERF isoforms and their colocalization with NHE3, ezrin, and ROMK. *Am. J. Physiol.* **280**, C192-C198.

Wegner, B., Al-Momany, A., Kulak, S. C., Kozlowski, K., Obeidat, M., Jahroudi, N., Paes, J., Berryman, M. and Ballermann, B. J. (2010). CLIC5A, a component of the ezrin-podocalyxin complex in glomeruli, is a determinant of podocyte integrity. *Am. J. Physiol.* **298**, F1492-F1503.

Yeung, T., Terebiznik, M., Yu, L., Silvius, J., Abidi, W. M., Philips, M., Levine, T., Kapus, A. and Grinstein, S. (2006). Receptor activation alters inner surface potential during phagocytosis. *Science* **313**, 347-351.

Yonemura, S., Tsukita, S. and Tsukita, S. (1999). Direct involvement of ezrin/radixin/moesin (ERM)-binding membrane proteins in the organization of microvilli in collaboration with activated ERM proteins. *J. Cell Biol.* **145**, 1497-1509.

Yonemura, S., Matsui, T., Tsukita, S. and Tsukita, S. (2002). Rho-dependent and -independent activation mechanisms of ezrin/radixin/moesin proteins: an essential role for polyphosphoinositides in vivo. *J. Cell Sci.* **115**, 2569-2580.

Zwaenepoel, I., Naba, A., Da Cunha, M. M., Del Maestro, L., Formstecher, E., Louvard, D. and Arpin, M. (2012). Ezrin regulates microvillus morphogenesis by promoting distinct activities of Eps8 proteins. *Mol. Biol. Cell* **23**, 1080-1095.